

Spin dependent transport phenomena in nanometer-sized heterostructures

Morten Høgsbro larsen

Anders Mathias Lunde

2nd May 2001

Niels Bohr Institute
University of Copenhagen
Denmark

Supervisors: Karsten Flensberg and Henrik Bruus

Preface

This bachelor thesis is written at the University of Copenhagen, Denmark, under the supervision of Karsten Flensberg and Henrik Bruus, both associated professors at the University of Copenhagen. We are thankful for all the work and time they have spent on us, and for the positive and inspiring way in which they supervised us.

The thesis is intended to have a level of difficulty so other 3rd year students without lots of problems can read it with only the skills obtained in undergraduate courses at the University of Copenhagen. However, because the course in solid state physics at the 3rd year is optional, and because the thesis naturally assumes some knowledge in this field, we cannot guarantee that every student will be familiar with all basic aspects.

The parts of the project dealing with giant magnetoresistance and spin-filtering, are made partly with Johan Chang and Jonas Nyvold Petersen, i.e. on the level of calculations and discussions the two groups have cooperated, but the writings are made separately. We thank them for inspiring discussions.

The two authors have contributed equally to the work in making the thesis. Both authors have read and contributed to every section and are as such equally responsible for every section.

Contents

Preface	I
1 Introduction	1
2 Giant MagnetoResistance in Fe-films with antiferromagnetic coupling	2
2.1 The model	3
2.2 Boundary conditions	4
2.3 The calculations	7
2.4 Results	8
2.5 Conclusion	10
2.6 Closing remarks	10
3 Quantum mechanical approach to spin filtering	11
3.1 The model	11
3.2 The Hamiltonian describing the system	12
3.3 The spin polarized current.	15
3.4 Conclusion.	16
4 The Rashba Hamiltonian	17
4.1 The Rashba Hamiltonian and its order of magnitude	17
4.2 Application of H_R to a system with Fe-magnets and a 2DEG. . .	18
4.3 Calculation of the transport properties	19
4.3.1 Eigenstates in the ferromagnets	19
4.3.2 Eigenstates in the 2DEG	20
4.3.3 Normalization of the eigenstates and derivation of the velocity operators.	21
4.3.4 Energy considerations and wave vectors	23
4.3.5 Transmission and reflection at the interfaces	24
4.3.6 Precession in the 2DEG	26
4.4 The conductance of the system.	27
4.5 Results and comments	27
4.6 A possible spin polarizer?	29
4.7 Conclusion	31
References	32
Appendix A The g-function's coefficients	34
Appendix B Calculation of the current density	35

1 Introduction

The goal with this thesis is to describe some simple and yet very interesting applications of spin dependent transport properties in certain media, such as nanometer-sized Fe|Cr|Fe-heterostructures or 2 dimensional electron gases (arising in the narrow gap between two semiconductors). What is basically interesting with this relatively new (and hot) subfield of solid state physics, called spintronics, is that the spin of the electron has become an important factor, instead of being just something that cannot be controlled.

The idea is to be able to transport or store information in the electronic spin. This would make it possible to use the electrons as the basic unit in a computer and thereby obtaining the so-called quantum computer [Hu]. This is the dream for the distant future and a lot of the technical details are yet to be overcome [Das]. Applications within range are electronic devices from ultra sensitive sensors in harddisks to spin filters to be used within the broad field of lasers [Egues].

A condition for this to make sense in the first place is that an electrons spin is not altered over length scales comparable with the system under consideration, so the electrons are able to “remember” their spin. This requirement can actually be met by choosing the right materials, because the spin mean-free path l_σ is extremely dependent on the band structure [Das] and the “record” is $0.1mm$ at $40K$ in aluminium [Prinz, p.60]. Generally l_σ is diminished at higher temperatures because of the phonon collisions [Das].

The way the spin of the electrons comes into play is primarily through the interaction with some magnetic field. This field can be caused by an external magnetic field, as is the case in the example with the spin filter, where the paramagnetic property of the system under consideration is exploited. It can also be introduced by an electric field as is the case in the Rashba-effect, which may arise in a 2 dimensional electron gas. Also, spin dependent quantum mechanical transmission coefficients through an interface can be the cause for the spin’s importance, as is the case in the example with giant magnetoresistance.

At the present state one hopes to explain some of the theoretical aspects of spintronics and spin dependent transport properties.

Throughout the text we will use the SI-system for the units unless otherwise specified.

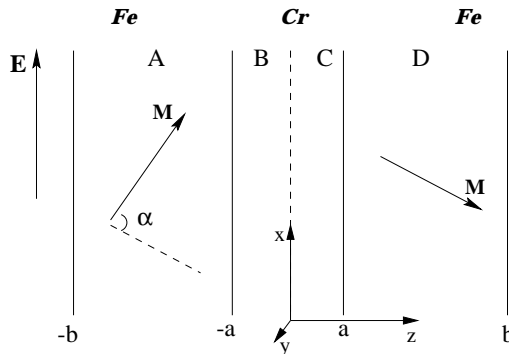


Figure 1: Geometry of the Fe|Cr|Fe-system which is divided into regions A,B,C and D. The angle α between the magnetizations in the two Fe-layers which is $\neq \pi$, when an external magnetic field is present.

2 Giant MagnetoResistance in Fe-films with anti-ferromagnetic coupling

Giant MagnetoResistance (GMR) is the description of the phenomenon that some (structures of) compounds show a large relative change in resistivity when an external magnetic field is applied. The cause for the slanted name is historical, i.e. GMR was discovered after “normal” magneroresistance (MR) and got its name simply because the effect was a lot bigger than that of MR [Prinz].

In this section we will show how GMR arises in a single nm -sized sandwich structure of Fe|Cr|Fe, based on [Barnas]. To this end we assume that the two metals are identical in several ways, i.e. that they have the same Fermi-energy, the same mean free path and that they are band gap matched, i.e. that there is no offset between the energy bands in the two metals. Only their magnetic properties are taken to be different. Consider first the geometry of the system shown in figure 1. In zero external magnetic field there exists an effective anti-ferromagnetic coupling between the two Fe-layers due to the intervening Cr-film. The explanation for this fact is out of the scope for this project. What is interesting is that an external magnetic field will be able to alter the configuration of the magnetizations in the Fe-films, so that the angle α between the magnetizations becomes an important parameter in the problem. What we would like to do is to study the resistivity of the system as a function of this angle (or in an actual experimental setup, the external field). To do this we imagine that an external electric field \mathbf{E} is applied to the system in the positive x direction, so as to drive a current in this direction. So we take $\mathbf{E} = (E_x, 0, 0)$ as seen in figure 1.¹

¹It may be shown that the effect we are going to describe can be even bigger for perpendicular transport [Prinz], but we will not consider that case.

2.1 The model

We adopt a semi-classical approach to describe the electrons in the metals. In this model the transport of electrons is described by the Boltzmann-equation, which in general is a rather complicated differential equation

$$\frac{\partial f}{\partial t} + \frac{d\mathbf{v}}{dt} \cdot \nabla_{\mathbf{v}} f + \mathbf{v} \cdot \nabla_{\mathbf{r}} f = \left(\frac{\partial f}{\partial t} \right)_{\text{collisions}} \quad (1)$$

where $f = f(\mathbf{r}, \mathbf{v})$ is the classical, non-equilibrium distribution function, i.e. $f(\mathbf{r}, \mathbf{v}) d\mathbf{r} d\mathbf{v}$ is the number of particles in the volume $d\mathbf{r} d\mathbf{v}$ about \mathbf{r}, \mathbf{v} . f_0 is f at thermal equilibrium, taken to stem from the Fermi-Dirac distribution (later, eq. (16), we show how the two are related). It may here be pointed out that it is actually reasonable to use this semi-classical approach in our problem because we are going to work with a small and constant external electrical field. This implies that the electrons, which are to be properly described by a wave packet extending over a number of primitive cells in the crystal structure, can safely be treated classically, because they have well defined wave-vectors on the length scale of the fields variations. So specifying \mathbf{r} and \mathbf{v} at the same time in $f(\mathbf{r}, \mathbf{v})$ does not violate the Heisenberg uncertainty relation principle $\Delta x \Delta p_x \geq \hbar/2$ on these length scales [Ashcroft & Mermin, p. 217].

To use the Boltzmann-equation, one must consider how to model the collisions of the electrons. One way to do this, which may be considered as the most simple, is the relaxation-time approximation, in which the electrons experience a collision in an infinitesimal time dt with probability dt/τ , and where the role of the collisions is to drive the system toward equilibrium. In this model the Boltzmann-equation reduces to

$$\frac{\partial f}{\partial t} + \frac{d\mathbf{v}}{dt} \cdot \nabla_{\mathbf{v}} f + \mathbf{v} \cdot \nabla_{\mathbf{r}} f = -\frac{f - f_0}{\tau} \quad (2)$$

where $\tau = \tau(\mathbf{r}, \mathbf{v})$ is the average time between collisions and is in general a function of \mathbf{r} and \mathbf{v} [Kittel, p.647-648]. In our model we take τ to be a constant. We define the difference from thermal equilibrium $g = f - f_0$ to simplify the equation.

In the case of steady state current ($\frac{\partial f}{\partial t} = 0$) and with $\frac{d\mathbf{v}}{dt} = \frac{-e}{m}(E_x, 0, 0)^2$ and $\nabla_{\mathbf{r}} f = (0, 0, \frac{\partial f}{\partial z})$, because we assume that the system is homogeneous in the xy plane, we have

$$\frac{-eE_x}{m} \frac{\partial f}{\partial v_x} + v_z \frac{\partial f}{\partial z} = -\frac{g}{\tau}.$$

Now $\frac{\partial f_0}{\partial z} = 0$ by definition of thermal equilibrium, and because we want linear response in the system upon E_x , we omit $\frac{\partial g}{\partial v_x}$ from $\frac{-eE_x}{m} \frac{\partial f}{\partial v_x}$, because g is itself

²Here we have omitted the magnetic field from the total force on the electron because its influence on the electron is negligible compared to the influence from the electric field.

at least linear in E and we would otherwise end up with a non-linear term in E . The Boltzmann equation therefore becomes

$$\frac{\partial g}{\partial z} + \frac{g}{\tau v_z} = \frac{e E_x}{m v_z} \frac{\partial f_0}{\partial v_x} \quad (3)$$

which is a differential equation in z for $g(\mathbf{r}, \mathbf{v})$. There is one such equation for each region, according to figure 1, so we divide g according to what region we consider.

We are now going to impose scattering conditions at the various boundaries. Because these are taken to be spin dependent, we calculate separately the contributions to g from spin-up and spin-down electrons, (it is of decisive importance that these contributions turn out not to be equal). Also, we divide g to describe separately electrons having positive and negative velocities in the z -direction. Thus for electrons in region A, moving in the positive z -direction, we get

$$g_{A+}(v_z, z) = g_{A+\uparrow}(v_z, z) + g_{A+\downarrow}(v_z, z)$$

and similarly for g_{A-} and for the other regions. Now, a solution to (3) is given by

$$g_{A\pm\uparrow}(v_z, z) = \frac{e E_x \tau}{m} \frac{\partial f_0}{\partial v_x} \left(1 + A_{\pm\uparrow} \exp\left(\frac{\mp z}{\tau |v_z|}\right) \right), \quad (4)$$

and similarly for the other regions and for spin-down electrons. The integration constants $A_{\pm\uparrow}, B_{\pm\uparrow}, C_{\pm\uparrow}, D_{\pm\uparrow}$ are to be determined by the boundary conditions.

2.2 Boundary conditions

At the outer boundaries $z = \pm b$, an incoming electron will have a certain probability R_0 to be reflected specularly (mirrorlike) and a certain probability to be reflected in a random direction, which we will call *diffuse reflection* [de Vries]. The electrons which are diffusely reflected tend to restore the thermal equilibrium, i.e. in average they will not contribute to g , the difference from equilibrium (see figure 2 on the following page). The distribution functions at the boundaries will therefore be related according to

$$\begin{aligned} g_{A+\uparrow} &= R_0 g_{A-\uparrow} \quad \text{at } z = -b \\ g_{D-\uparrow} &= R_0 g_{D+\uparrow} \quad \text{at } z = +b. \end{aligned}$$

and similarly for the spin-down electrons. However, according to [de Vries], it is an reasonable simplification to assume that $R_0 = 0$, so that every electron hitting the boundary will be scattered diffusely and there will be thermal equilibrium

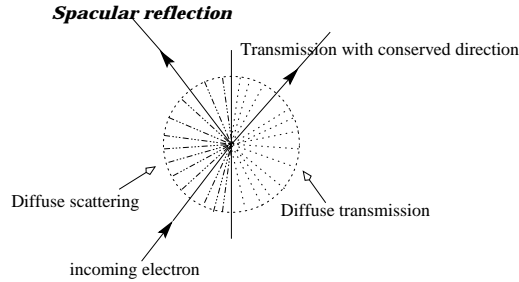


Figure 2: The difference between diffuse and specular scattering

right at the outer boundaries. This determines $A_{+\uparrow} = A_{+\downarrow} = D_{-\uparrow} = D_{-\downarrow} = -\exp(\frac{-b}{\tau|v_z|})$.

At the interfaces between the Fe- and Cr-layer, there is also in general both reflection and transmission for an incoming electron, where the reflection and transmission can be specular or diffuse. Again it is reasonable to assume that there is no specular reflection, and because diffusely scattered electrons in average do not contribute to g , we consider only electron transmission which conserves the direction of the incoming electron (see figure 2). Therefore we can describe the scattering at the interfaces by only the spin dependent diffuse scattering³ coefficients \mathcal{D}_{\uparrow} and \mathcal{D}_{\downarrow} , and the transmission to be considered is $1 - \mathcal{D}_{\uparrow}$ for the spin-up electrons and $1 - \mathcal{D}_{\downarrow}$ for the spin-down electrons. These two parameters are not equal, which is what basically gives rise to the magnetoresistance effect. We define $N = \frac{\mathcal{D}_{\uparrow}}{\mathcal{D}_{\downarrow}}$. At the interfaces we now have relations between the various g 's:

$$g_{A-\uparrow} = (1 - \mathcal{D}_{\uparrow})g_{B-\uparrow} \quad \text{at } z = -a \quad (5)$$

$$g_{B+\uparrow} = (1 - \mathcal{D}_{\uparrow})g_{A+\uparrow} \quad \text{at } z = -a, \quad (6)$$

and similarly for the spin down and at $z = +a$, i.e. there are 6 more equations like this.

Introducing the angle α between the magnetizations (see figure 1 on page 2) in the two Fe-films, we can now describe the boundary conditions at $z = 0$. When passing from A to D (or from D to A), we change the basis for the spin space, because the electrons spin is to be described relatively to the magnetization in the region where it is. Taking this change to occur exactly at $z = 0$ is of course an approximation, because in reality the change in magnetization takes place in a continuous way through the Cr-layer. Now, for a general orientation (not necessarily in the xz -plane) of the magnetizations we define a new coordinate system with the origin coinciding with the old, but with the $x'z'$ -plane defined as the plane spanned by the two magnetizations and the y' -axis perpendicular to

³The diffuse scattering coefficient is the sum of the diffuse reflection and diffuse transmission coefficients.

this plane so as to define a right-handed system.⁴ According to general quantum mechanical principles for rotations of spinors, (e.g. [Sakurai, p.166]) we have for a general spinor $\begin{pmatrix} c_{A+} \\ c_{A-} \end{pmatrix}$ in A that the corresponding spinor in D for a rotation about the y' -axis, is

$$\begin{pmatrix} c_{D+} \\ c_{D-} \end{pmatrix} = \begin{pmatrix} \cos(\frac{\alpha}{2}) & -\sin(\frac{\alpha}{2}) \\ \sin(\frac{\alpha}{2}) & \cos(\frac{\alpha}{2}) \end{pmatrix} \begin{pmatrix} c_{A+} \\ c_{A-} \end{pmatrix}$$

With this equation we get for a spin-up electron, $\begin{pmatrix} 1 \\ 0 \end{pmatrix}$ at $z = -0$ that the spin-down part of it, $\begin{pmatrix} 0 \\ 1 \end{pmatrix}$ at $z = +0$ is $T_{\uparrow\downarrow} = \sin^2(\alpha/2)$ and that the spin-up part is $T_{\downarrow\uparrow} = \cos(\alpha/2)$. With this notation, we have

$$T_{\uparrow\uparrow} = T_{\downarrow\downarrow} = \cos^2(\alpha/2) \quad (7)$$

$$T_{\uparrow\downarrow} = T_{\downarrow\uparrow} = \sin^2(\alpha/2) \quad (8)$$

(which is seen by inspection to be valid also in the limiting cases, $\alpha = 0, \pi$) and the “boundary” conditions at $z = 0$ become

$$g_{C+\uparrow} = T_{\uparrow\uparrow}g_{B+\uparrow} + T_{\uparrow\downarrow}g_{B+\downarrow} \quad (9)$$

$$g_{C+\downarrow} = T_{\downarrow\downarrow}g_{B+\downarrow} + T_{\downarrow\uparrow}g_{B+\uparrow} \quad (10)$$

and similarly for $g_{B-\uparrow}$ and $g_{B-\downarrow}$. The equations (5), (6), (9), (10) and the two equations for $g_{B-\uparrow}$ and $g_{B-\downarrow}$ together with (7) and (8), now give⁵ us the remaining integration coefficients, one of which is⁶

$$B_{+\uparrow} = \left[\left(1 - \exp\left(\frac{a-b}{\tau|v_z|}\right) \right) (1 - \mathcal{D}_{\uparrow}) - 1 \right] \exp\left(\frac{-a}{\tau|v_z|}\right),$$

and the others being similar or slightly more complicated. a and b are the dimension parameters according to figure 1.

Now we have found all the g 's (the coefficients just have to be substituted in (4)), and it is seen that they are functions only of the parameters \mathcal{D}_{\uparrow} and \mathcal{D}_{\downarrow} . So we are now in a position where we can find the current density in the various regions, by performing the integration

$$J = \int_{\text{region}} \int_{\text{all } \mathbf{v}'s} ev_x g(v_z, z) d\mathbf{v} dz \quad (11)$$

where the integration with respect to z is to be split up according to the several regions.

⁴If the magnetizations are not linearly independent, which will be the case for zero magnetic field, this construction obviously fails, but we will see that the limiting result for this case is in accordance with what one should expect from first principles, i.e. that a spin-up (spin-down) electron entering another region will certainly be a spin-down (spin-up) electron if the magnetizations are anti-parallel.

⁵By tedious solving of linear equations.

⁶The rest can be seen in appendix A.

2.3 The calculations

The integral for the electrons with positive velocity in A is explicitly:

$$J = \frac{e^2 E_x \tau}{m} \int_{-b}^{-a} \int_{\text{all } \mathbf{v}'_s} v_x \frac{\partial f_0}{\partial v_x} \left(2 + (A_{+\uparrow} + A_{+\downarrow}) \exp\left(\frac{-z}{\tau|v_z|}\right) \right) d\mathbf{v} dz \quad (12)$$

To evaluate this and the other similar integrals in practice, several modifications need to be done. First we make a change of variables for the velocity integral into polar coordinates in the velocity space. Now, working at room temperature⁷ and changing the velocity integral into an energy integral would enable us to substitute the factor $\frac{\partial f_0}{\partial v_x}$, appearing in the integrals with a Dirac delta function in the energy, *if* f_0 were the Fermi-Dirac distribution, because this latter approaches a unit step function when the temperature goes to zero ([Kittel, p.147]). But f_0 is a classical distribution function, describing the distribution of particles in a (modified) *phase space* (\mathbf{v} in stead of \mathbf{p}), and not the distribution of particles in quantum states (like the Fermi-Dirac distribution), so we have to find the connection between these two ways to express the same thing.

To do this, we consider the problem of finding the thermal equilibrium average of a quantity $X = X(|\mathbf{v}|)$ using the two different distribution functions. The results must be equal. Using the classical distribution f^c one should write

$$\langle X(|\mathbf{v}|) \rangle = \int_{\text{all } \mathbf{v}'_s} X(|\mathbf{v}|) f^c(|\mathbf{v}|) d^3 \mathbf{v} \quad (13)$$

By doing the integration in polar coordinates we obtain (the 4π comes from the ϕ and θ integration)

$$\langle X(|\mathbf{v}|) \rangle = 4\pi \int_0^\infty v^2 X(|\mathbf{v}|) f^c(|\mathbf{v}|) dv = 4\pi \int_0^\infty \sqrt{\frac{2\varepsilon}{m^3}} X(v_\varepsilon) f^c(v_\varepsilon) d\varepsilon \quad (14)$$

where we have converted the integral over v into an energy integral, using $\varepsilon = \frac{1}{2}mv^2$.

By using the Fermi-Dirac distribution f^{FD} one should write

$$\langle X(|\mathbf{v}|) \rangle = \int_0^\infty f^{\text{FD}}(\varepsilon) \mathcal{D}(\varepsilon) X(\varepsilon) d\varepsilon \quad (15)$$

where $\mathcal{D}(\varepsilon)$ is the density of states for a free 3-dimensional electron gas and is found from the number N of one particle orbitals of energy less than or equal to ε as ([Kittel, p.149])

$$\mathcal{D}(\varepsilon) = \frac{dN}{d\varepsilon} = \frac{V}{2\pi^2} \left(\frac{2m}{\hbar^2} \right)^{3/2} \varepsilon^{1/2}$$

⁷Room temperature is much less than the Fermi temperature for the metals, which is typically of the order of 10^4

By equating (14) and (15) we obtain

$$f^c(v_\varepsilon) = f^{\text{FD}} \frac{Vm^3}{4\pi^3\hbar^3} \quad (16)$$

Putting all this together, i.e. changing the integration over $|\mathbf{v}|$ into an energy integral by substituting $\varepsilon = \frac{1}{2}m(v_x^2 + v_y^2 + v_z^2)$ and using the result from (16), remembering that $\frac{\partial f^{\text{FD}}}{\partial \varepsilon} = \delta(\varepsilon - \varepsilon_F)$, we have from (12):

$$\frac{\partial f_0}{\partial v_x} dv = \frac{\partial f_0}{\partial \varepsilon} \frac{v_x}{v} d\varepsilon = \frac{m^3}{4\pi^3\hbar^3} \delta(\varepsilon - \varepsilon_F) \sin(\theta) \cos(\phi) d\varepsilon,$$

where ε_F is the Fermi energy.⁸

Doing the energy integration (over the delta function), inserts the values of the several variables at ε_F , and we are now left with (for the electrons moving in the positive z -direction in region A)

$$J = \frac{m^2 e^2 \tau E_x}{4\pi^3 \hbar^3} 2\pi v_F^3 \int_{-b}^{-a} dz \int_0^\pi d\theta \sin^2(\theta) \left(2 + (A_{+\uparrow} + A_{+\downarrow}) \exp\left(\frac{-z}{\lambda \cos(\theta)}\right) \right) \quad (17)$$

and similar integrals in the other regions. v_F is the velocity at the Fermi energy and the mean free path λ has been introduced as an approximation for τ by $\lambda = \tau v_F$. Now, also the current density of electrons moving in the negative z -direction are to be concerned, but because the part of the system not concerning magnetizations and spin exhibits a 180° rotation symmetry, this is the same as for the electrons moving in the positive direction. The total current density is thus twice the value obtained by (17). These integrals were evaluated by *Mathematica*, where it turned out to be very tough for the computer to do, unless the z -integration was done before the θ -integration and the integrands were expanded as much as possible to overcome problems concerning partial integration.

The resistivity can now easily be found using Ohm's law $J = \sigma E$ and the definition $\rho = \frac{1}{\sigma}$ (assuming isotropic conductivity).

2.4 Results

In figure 3(a), we show how the maximum resistivity changes as a function of \mathcal{D}_\uparrow and $N = \frac{\mathcal{D}_\uparrow}{\mathcal{D}_\downarrow}$. It is seen that the effect is of the order of some percent. The figure shows that the effect on the resistivity grows with N and \mathcal{D}_\uparrow , which means that both $\frac{\mathcal{D}_\uparrow}{\mathcal{D}_\downarrow}$ and the absolute value of \mathcal{D}_\uparrow are important parameters in the setup and should be specified with care. The parameter N has to be measured

⁸We have omitted V from this equation, because we are calculating the current density and we are therefore in fact using f^c/V from (14) as f_0 . We can do this because we can always consider f^c in as small a volume V as necessary.

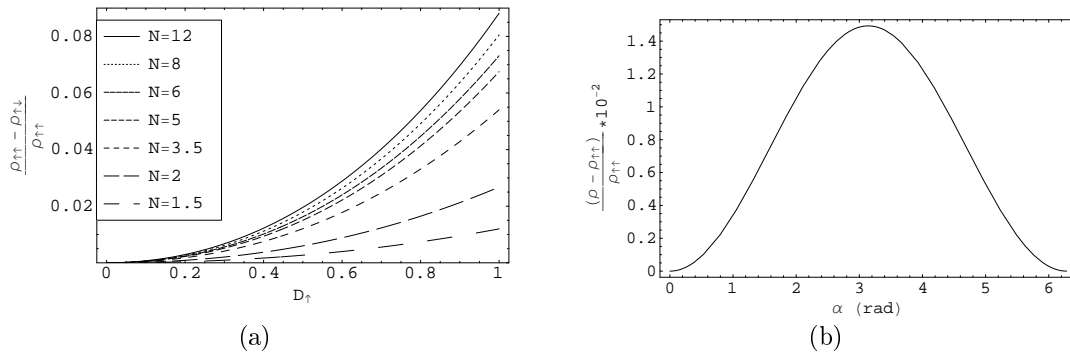


Figure 3: (a) The maximum relative change in resistivity as a function of \mathcal{D}_{\uparrow} . $\rho_{\uparrow\uparrow}$ is the resistivity for $\alpha = 0$, and $\rho_{\uparrow\downarrow}$ the resistivity for $\alpha = 180^\circ$. (b) The relative change in resistivity as a function of the angle between the magnetizations in the Fe-layers for $N = 6$ and $\mathcal{D}_{\uparrow} = 0.48$. In an actual experimental setup, the resistivity would be measured as a function of the applied field. To compare experiments and theory, one must therefore find the functional dependency of the angle on the applied field [Barnas, p.666].

experimentally, but some evidence, both experimentally and theoretically, exists [Barnas, p.666], that N should be about 6. Furthermore, \mathcal{D}_{\uparrow} being a measure for the roughness of the interfaces, is found experimentally. In figure 3(b) we have plotted the resistivity as a function of the angle α between the magnetizations in the two Fe-layers for $N = 6$ and $\mathcal{D}_{\uparrow} = 0.48$, where the value for \mathcal{D}_{\uparrow} is obtained in [Barnas] by fitting to experimental results.

It is seen that the relative change in resistivity is largest when the magnetizations are antiparallel ($\alpha = \pi$) and that the resistivity change for this case is about 1.4 percent. The results are in quite good agreement with experimental results shown in ([Barnas]). The figures 3(a) and 3(b) are for $a = 125\text{\AA}$, $b = 5\text{\AA}$, i.e. the calculation is for a $(120\text{\AA Fe})|(10\text{\AA Cr})|(120\text{\AA Fe})$ sandwich structure, and we take $\lambda = 180\text{\AA}$. One last parameter which it could be interesting to vary is the mean free path λ which we until now have taken to be 180\AA , a number appropriate to room temperature. But the model will be valid in a temperature interval, which is limited primarily by the approximation $\lambda = \tau v_F$. Because this approximation becomes better at low temperatures, we can safely consider longer mean free paths. The plot for the resistivity change as a function of λ is shown in figure 4. It shows that the maximum change in resistivity grows with λ (decreasing temperature) and that the most dramatic change occurs in the low temperature limit. This result is also in agreement with experimental values, according to [Barnas].

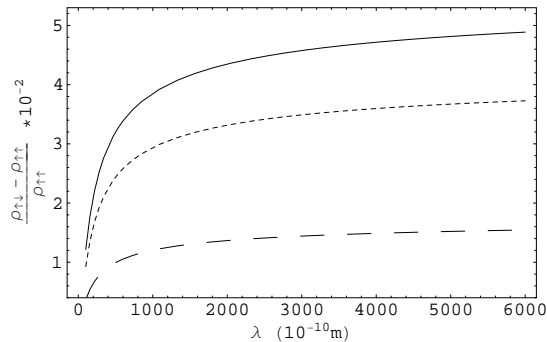


Figure 4: Relative change in the maximum resistivity as a function of the mean free path λ measured in \AA for three different combinations of \mathcal{D}_\uparrow and N :
 (—) $\mathcal{D}_\uparrow = 0.5, N = 12$; (\cdots) $\mathcal{D}_\uparrow = 0.48, N = 6$; (---) $\mathcal{D}_\uparrow = 0.5, N = 2$

2.5 Conclusion

We have shown how there can be a change in the resistivity for a Fe|Cr|Fe sandwich structure as a function of the relative orientation of the magnetizations in the Fe-layers. We based our model on the semi-classical model for the electrons in the metals, and imposed spin-dependent scattering conditions at the boundaries and the interfaces.

2.6 Closing remarks

The effect considered in this section is of the order of some percent, but can be extended by considering a lattice structure consisting of many (on the order of 10^2) layers in stead of a single sandwich structure, thereby obtaining changes of about 100% or more [Barnas]. Noteworthy, GMR has come to use in the computer technology as sensors in harddisks where the ever growing demand for greater density of stored data leads to the development of more sensible sensors [IBM].

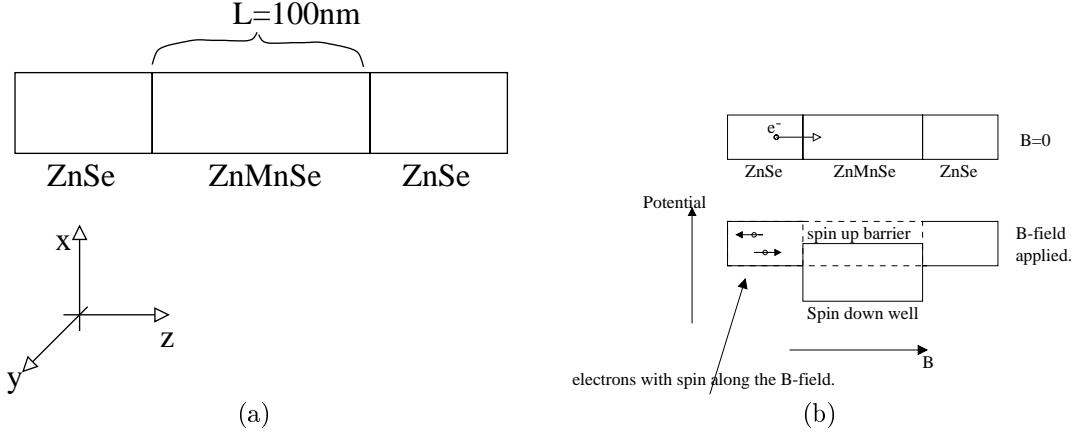


Figure 5: (a) The geometry for the spinfilter structure. (b) The potential difference for the spin-up and spin-down electrons in the $\text{Zn}_{1-x}\text{Mn}_x\text{Se}$ layer on a relative scale.

3 Quantum mechanical approach to spin filtering

3.1 The model

In this section we describe a model for spin filtering of an electrical current. It is based on quantum mechanical scattering of electrons on a rectangular potential, and was first proposed by J.C.Egues [Egues]. We will try to emphasize the quantum mechanical nature of this problem. We consider a $\text{ZnSe}|\text{Zn}_{1-x}\text{Mn}_x\text{Se}|\text{ZnSe}$ sandwich heterostructure as in figure 5(a), where we model a perpendicular current (as opposed to the current in the GMR section), i.e. the current is in the z -direction. It turns out that the current will be spin polarized in the presence of an external magnetic field (of about 2-3T), i.e. the current will consist of electrons with only one spin orientation.

The cause for the difference in spin-up and spin-down current is the *exchange interaction* between the conduction electrons and the electrons in the Mn^{2+} -ions. The exchange interaction is a purely quantum mechanical effect, occurring because the electrons are fermions and therefore obey the Pauli principle. Now in the $\text{ZnSe}|\text{Zn}_{1-x}\text{Mn}_x\text{Se}|\text{ZnSe}$ structure some of the Zn^{2+} -ions in the middle layer are replaced by Mn^{2+} -ions. Mn^{2+} -ions have the electron configuration $(\text{Ar})3d^5$. By applying Hund's rule⁹ we see that all the electrons in the outer shell of Mn^{2+} -ions have the same spin orientation, making the $\text{Zn}_{1-x}\text{Mn}_x\text{Se}$ -layer paramagnetic (in comparison the ZnSe -layer is non-magnetic, Zn^{2+} and Se^{2-} having the config-

⁹Hund's rule states how the electrons distribute in an atom or ion in its ground state, i.e. it gives the S, l and J quantum numbers, given the principal quantum number n . In this case we get $S = J = \frac{5}{2}$ and $l = 0$. [Kittel, p.424]. Hund's rule may be seen as a compact way of expressing the Pauli exclusion principle, the Coulomb interaction and the spin-orbit coupling at once.

urations (Ar) $3d^{10}$ and (Ar) $4s^24p^6$). By applying an external magnetic field, the Mn^{2+} -ions will tend to anti-align their spins to the magnetic field but align them to each other, thereby giving rise to a potential difference for spin-up and spin-down conduction electrons: when a conduction electron with its spin aligned like the electrons in the Mn^{2+} -ions approaches the ions, the exchange energy grows, whereas for an electron with its spin anti-aligned with the ions the exchange energy falls off, see figure 5(b) on the page before¹⁰.

The basic assumptions in the model are that the electrons are mutual non-interacting, that there is no overlap of the energy bands in either of the metals and that there is no electron scattering on the lattice. We further assume that the concentration of the Mn^{2+} -ions is small (5%) and that we work at low temperatures (5K).

The $\text{ZnSe}|\text{Zn}_{1-x}\text{Mn}_x\text{Se}|\text{ZnSe}$ structure was chosen because with $x = 0.05$ it is band-gap matched (i.e. the offsets of the valence and conduction bands in the different layers are taken to be zero), so the conduction electrons feels no interfaces in the heterostructure when zero magnetic field is applied (see figure 5(b)).

3.2 The Hamiltonian describing the system

We will now find the Hamiltonian for one electron in the heterostructure. This is the relevant Hamiltonian for the problem, because we assumed independent electrons, so in the end the total wavefunction will be given as a product of single electron wavefunctions. Because we also ignored the electron scattering on the crystal structure, we obtain (except for the spin interaction) the Hamiltonian as:

$$\hat{H} = \frac{1}{2m_e^*}(\hat{\mathbf{p}} - e\mathbf{A})^2 = \frac{1}{2m_e^*}((\hat{p}_x + \frac{1}{2}eBy)^2 + (\hat{p}_y - \frac{1}{2}eBx)^2 + \hat{p}_z^2) \quad (18)$$

Here m_e^* is the effective mass of the electron (assumed equal in the two layers), $|\mathbf{B}| = B$ and we have used the gauge freedom [Griffiths, p. 429] to choose $\mathbf{A} = (-\frac{1}{2}By, \frac{1}{2}Bx, 0)$ so $\mathbf{B} = \nabla \times \mathbf{A}$ is along the z -axis. This Hamiltonian shows that motion in the z -direction is not coupled to the motion in the xy -plane. The energy of the xy motion is quantized in the Landau levels $E_n = \hbar\omega_c(\frac{1}{2} + n)$ where n is a nonnegative integer and $\omega_c = \frac{eB}{m_e^*}$ is called the cyclotron frequency [Liboff, p. 442]. The motion in the z direction is represented by plane wave states $e^{ik_z z}$ with energy $E_z = \frac{\hbar^2 k_z^2}{2m_e^*}$. This makes it possible to use *one dimensional* potentials in this direction to describe the system and the cause for the spin filtering.

First we derive these potentials and see how they become rectangular. The general interaction between the spin $\hat{\boldsymbol{\sigma}} = (\hat{\sigma}_x, \hat{\sigma}_y, \hat{\sigma}_z)$ of the conduction electron

¹⁰For the conduction electrons we measure “up”- and “down”-spin relative to the average alignment of the Mn^{2+} -ions

and a single Mn^{2+} -ion spin $\hat{\boldsymbol{\sigma}}_{\text{Mn}^{2+}} = (\hat{\sigma}_{x,\text{Mn}^{2+}}, \hat{\sigma}_{y,\text{Mn}^{2+}}, \hat{\sigma}_{z,\text{Mn}^{2+}})$ is $\hat{V}_{\text{single ion}} = c\hat{\boldsymbol{\sigma}}_{\text{Mn}^{2+}} \cdot \hat{\boldsymbol{\sigma}}$ where c is a constant. This is the dominant interaction for the electron spin in the heterostructure. This operator acts on the system consisting of an electron and a Mn^{2+} -ion, i.e. on a superposition of $|SM_S\rangle_{\text{Mn}^{2+}}|sm_s\rangle_{e^-}$ states. This means that $\hat{V}_{\text{single ion}}$ is not (like equation (18)) a Hamiltonian for a single conduction electron alone, and before we can use them together to describe the energy of the electron, we have to make it independent of the ions. The total interaction in the structure for one conduction electron spin $\hat{\boldsymbol{\sigma}}$ and the Mn^{2+} -ions is (because we assumed low concentration x and thereby neglecting the small ion-ion interaction [Ashcroft & Mermin, p. 681]):

$$\hat{V}_{\text{spin}} = \sum_i c_i \hat{\boldsymbol{\sigma}}_{i,\text{Mn}^{2+}} \cdot \hat{\boldsymbol{\sigma}} \quad (19)$$

where the sum is over the Mn^{2+} -ions in the lattice. We now make a mean field approximation for the Mn^{2+} -ions, so that for all i , $\hat{\boldsymbol{\sigma}}_{i,\text{Mn}^{2+}} = (\hat{\sigma}_{ix}, \hat{\sigma}_{iy}, \hat{\sigma}_{iz})$ becomes $\langle \hat{\boldsymbol{\sigma}}_{\text{Mn}^{2+}} \rangle = (\langle \hat{\sigma}_x \rangle, \langle \hat{\sigma}_y \rangle, \langle \hat{\sigma}_z \rangle)$. Here $\langle \hat{\sigma}_x \rangle = \langle \hat{\sigma}_y \rangle = 0$ because the magnetic field is in the z -direction, which implies that the x and y components of the Mn^{2+} -spins are randomly oriented.

Equation (19) can also be written as

$$\hat{V}_{\text{spin}} = \sum_i c_i \left(\frac{1}{2} (\hat{\sigma}_{i-, \text{Mn}^{2+}} \hat{\sigma}_+ + \hat{\sigma}_{i+, \text{Mn}^{2+}} \hat{\sigma}_-) + \hat{\sigma}_{iz, \text{Mn}^{2+}} \hat{\sigma}_z \right) \quad (20)$$

by using lowering and raising operators [Liboff, p.528]. This shows that \hat{V}_{spin} gives rise to transition between spin states (spin flips). By making the mean field approximation we ignore the possibility for spin flips.

In the mean field approximation the interaction becomes:

$$\begin{aligned} \hat{V}_{\text{spin}} &\simeq \sum_i c_i \langle \hat{\boldsymbol{\sigma}}_{i,\text{Mn}^{2+}} \rangle \cdot \hat{\boldsymbol{\sigma}} = \sum_i c_i \langle \hat{\sigma}_{z,\text{Mn}^{2+}} \rangle \hat{\sigma}_z \\ &= \langle \hat{\sigma}_{z,\text{Mn}^{2+}} \rangle \hat{\sigma}_z \sum_i c_i = \langle \hat{\sigma}_{z,\text{Mn}^{2+}} \rangle \hat{\sigma}_z N_0 \alpha x \end{aligned} \quad (21)$$

Here $N_0 \alpha$ is called the exchange constant and x is the Mn^{2+} concentration. We defined $\sum_i c_i = x N_0 \alpha$ which is reasonable because the greater concentration, the greater the interaction. This potential can now be seen as an operator for a single conduction electron only and as it is present in the $\text{Zn}_{1-x}\text{Mn}_x\text{Se}$ layer only, we have as a function of z :

$$\hat{V}_{\sigma_z}(z) = x N_0 \alpha \langle \hat{\sigma}_{z,\text{Mn}^{2+}} \rangle \hat{\sigma}_z \theta(z) \theta(L - z). \quad (22)$$

Here

$$\theta(z) = \begin{cases} 0 & \text{for } z < 0 \\ 1 & \text{for } z \geq 0 \end{cases}$$

is the unit step function, and L is the length of the $\text{Zn}_{1-x}\text{Mn}_x\text{Se}$ -layer.

The only dependence of the B -field in $\hat{V}_{\sigma_z}(z)$ is through $\langle \hat{\sigma}_{z,\text{Mn}^{2+}} \rangle$ and it is found by considering the magnetization M . The fraction of Mn^{2+} -ions in a given state m_s is $\frac{N_{m_s}}{N_{tot}} = \frac{\exp(-\varepsilon_{m_s}/k_bT)}{Z}$, where Z is the partition function and N_{tot} is the total number of Mn^{2+} -ions. The energy is $\varepsilon_{m_s} = -\bar{\boldsymbol{\mu}} \cdot \bar{\mathbf{B}} = -\mu_z B = m_s g \mu_B B$ expressed in the Bohr magneton $\mu_B = \frac{e\hbar}{2m_e}$, the magnetic quantum number m_s and the dimensionless Landé factor g . The magnetization is now found:

$$M = \sum_{m_s=-\frac{5}{2}}^{\frac{5}{2}} N_{m_s} (-g \mu_B m_s) = \frac{5}{2} N_{tot} g \mu_B \mathcal{B}_{\frac{5}{2}}(\gamma) \quad (23)$$

where¹¹

$$\mathcal{B}_{\frac{5}{2}}(\gamma) = \frac{6}{5} \coth\left(\frac{6\gamma}{5}\right) - \frac{1}{5} \coth\left(\frac{\gamma}{5}\right) \quad (24)$$

is a $\frac{5}{2}$ Brillouin function and where we have defined $\gamma = \frac{5g\mu_B B}{2k_bT}$ to simplify ([Kittel, p.417-422] and [Ashcroft & Mermin, p.655-656]).

On the other hand we must have that $M = N_{tot} \langle \boldsymbol{\mu}_{\text{Mn}^{2+}} \rangle$, where $\langle \boldsymbol{\mu}_{\text{Mn}^{2+}} \rangle$ is the thermal average of the Mn^{2+} magnetic moments. $\boldsymbol{\mu}_{\text{Mn}^{2+}}$ is given by $\boldsymbol{\mu}_{\text{Mn}^{2+}} = -\frac{g\mu_B}{\hbar} \hat{\mathbf{S}}_{\text{Mn}^{2+}} = -\frac{g\mu_B}{2} \hat{\boldsymbol{\sigma}}_{\text{Mn}^{2+}}$, where $\hat{\mathbf{S}}$ is the Mn^{2+} -ion spin. This means that $\langle \boldsymbol{\mu}_{\text{Mn}^{2+}} \rangle = -\frac{g\mu_B}{2} \langle \hat{\boldsymbol{\sigma}}_{\text{Mn}^{2+}} \rangle$ and as earlier noted $\langle \hat{\sigma}_{x,\text{Mn}^{2+}} \rangle = \langle \hat{\sigma}_{y,\text{Mn}^{2+}} \rangle = 0$, so $\langle \boldsymbol{\mu}_{\text{Mn}^{2+}} \rangle = -\frac{g\mu_B}{2} \langle \hat{\sigma}_{z,\text{Mn}^{2+}} \rangle$, which gives the expression $M = -N_{tot} \frac{g\mu_B}{2} \langle \hat{\sigma}_{z,\text{Mn}^{2+}} \rangle$. We can now obtain $\langle \hat{\sigma}_{z,\text{Mn}^{2+}} \rangle$ as a function of B :

$$M = -N_{tot} \frac{g\mu_B}{2} \langle \hat{\sigma}_{z,\text{Mn}^{2+}} \rangle = \frac{5}{2} N_{tot} g \mu_B \mathcal{B}_{\frac{5}{2}}(\gamma) \Rightarrow \langle \hat{\sigma}_{z,\text{Mn}^{2+}} \rangle = -5 \mathcal{B}_{\frac{5}{2}}(\gamma) \quad (25)$$

The only thing we now need to determine in $\hat{V}_{\sigma_z}(z)$ is the g -factor. This is found by the general formula for a free atom or ion [Kittel, p.420]: $g = \frac{3}{2} + \frac{S(S+1) - l(l+1)}{2J(J+1)} = 2$, because Hund's rule gave us $S = J = \frac{5}{2}$ and $l = 0$.

So we have now derived the spin interaction to be:

$$\hat{V}_{\sigma_z}(z) = -x N_0 \alpha 5 \mathcal{B}_{\frac{5}{2}}(\gamma) \hat{\sigma}_z \theta(z) \theta(L - z) \quad (26)$$

where [Egues] uses $N_0 \alpha = \frac{1}{4} 0.26 eV$ and $T = 5K$ in the calculations. The concentration used is $x_{\text{effective}} = x(1-x)$ ¹² with $x = 0.05$ to account for Mn^{2+} - Mn^{2+} -ion spin interaction.¹²

¹¹The second = in (23) requires some algebra

¹²These values were not present in the article, but were given to us by J.C. Egues himself. (He actually gave us $N_0 \alpha = 0.26 eV$, but due to his notation inconsistency regarding \mathbf{S} and $\boldsymbol{\sigma}$ we changed it.)

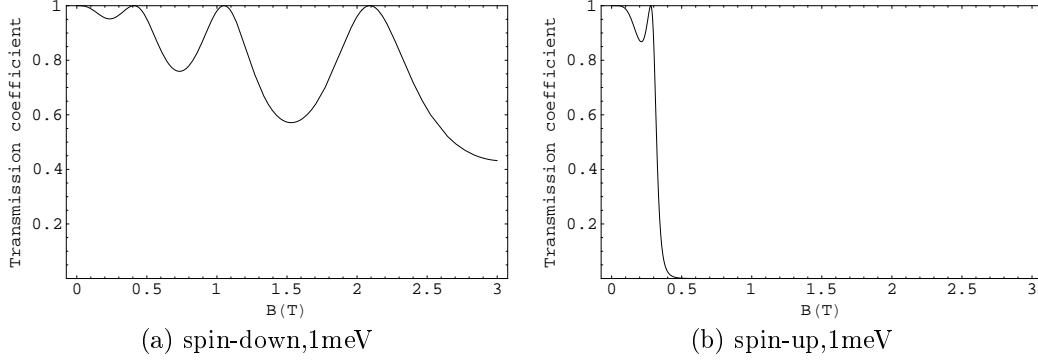


Figure 6: The transmission coefficients for (a) spin down and (b) spin up electrons versus B /Tesla for $E_z = 1meV$

3.3 The spin polarized current.

Now we know the full Hamiltonian, which gives rise to Landau quantization in the xy plan and a one dimensional scattering problem on a rectangular potential in the z -direction, where the potential is different for the two spin directions. This is what essentially gives the spin filtering.

In the one dimensional motion along the B -field we have plane wave states $e^{ik_z z}$ with energy $E_z = \frac{\hbar^2 k_z^2}{2m_e^*}$. The rectangular potential in the ZnMnSe layer now makes it possible to use known quantum mechanical transmission coefficients appropriate for such problems. The spin up electrons have potential energy $V_\uparrow = xN_0\alpha 5\mathcal{B}_{\frac{5}{2}}(\gamma)$, so the transmission coefficients for $V_\uparrow < E_z$ is:

$$T_\uparrow(E_z, B) = \left(1 + \frac{25}{4} \frac{(xN_0\alpha \mathcal{B}_{\frac{5}{2}}(\gamma))^2}{E_z(E_z + 5xN_0\alpha \mathcal{B}_{\frac{5}{2}}(\gamma))} \sin^2 \left(\sqrt{\frac{2m_e^*(E_z + 5xN_0\alpha \mathcal{B}_{\frac{5}{2}}(\gamma))^2}{\hbar^2}} L \right) \right)^{-1} \quad (27)$$

Similar expressions can be obtained for $T_\uparrow(E_z, B)$ for $V_\uparrow > E_z$ and for $T_\downarrow(E_z, B)$ ([Liboff, table 7.2 or section 7.6-8]). These transmission coefficients are plotted by *Mathematica* in figure 6 and 7 as a function of the B field at a given energy E_z . For spin up electron transmission we see the resonances (i.e. $T = 1$) whenever $\sin^2(k_z L) = 0$ or, with $k_z = \frac{2\pi}{\lambda_z}$ being the wave vector in the ZnMnSe layer, whenever $m \frac{\lambda_z}{2} = L$, i.e. an integral number of half-wavelength fit into the system. The difference for spin-up and spin-down transmission for $E_z = 5meV$ (figure 7 on the following page) shows that it is in theory possible to control by the external B -field the amount of spin up/down that you let through the system. It is seen

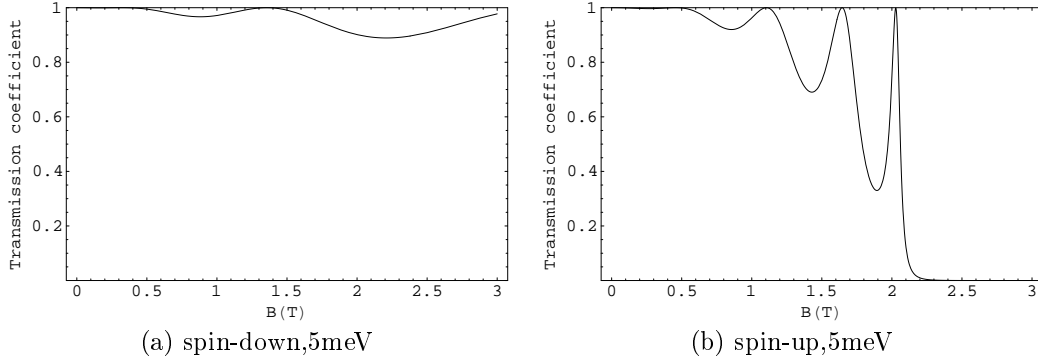


Figure 7: The transmission coefficients for (a) spin down and (b) spin up electrons versus B /Tesla for $E_z = 5meV$

that for $B > 2T$ the current consists only of spin down, i.e. we have a totally spin polarized current! Therefore we have constructed, in principle, a spin filter and the currents can be calculated by the same means as in the GMR section under the assumption of low temperatures. It is intuitively clear that the currents essentially will reflect the transmission coefficients, so actually all the important information about the spin filtering is shown in these.

3.4 Conclusion.

We have now shown that by the means of a simple quantum mechanical model using a 1-dimensional, rectangular scattering potential, we can construct a spin filter. An actual experimental setup that can give rise to the difference in energy for spin-up and spin-down electrons (and thereby in transmission coefficients) could be a layered heterostructure of the form $ZnSe|Zn_{1-x}Mn_xSe|ZnSe$. It is the exchange interaction between the electrons and the Mn^{2+} -ions, $\widehat{\mathbf{S}}_{Mn^{2+}} \cdot \widehat{\boldsymbol{\sigma}}_e$ that is the basic physical property explaining this. This interaction's strength depends in the mean field approximation on the net alignment of the magnetic moments of the Mn^{2+} -ions, which can be controlled by changing an external magnetic field.

As mentioned, by introducing the mean field approximation, we ignore the possibility for spin-flip due to the actual magnetization. This effect will tend to make our results less noticeable because of the mixing of spin-up and spin-down. Also, imperfections in the doping of ZnSe by Mn will cause the potential barriers to be less well defined and again the results will be less pronounced and the current will be less polarized.

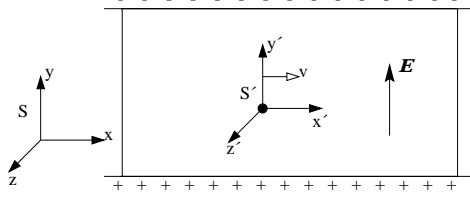


Figure 8: The system in which we derive the spin-orbit coupling.

4 The Rashba Hamiltonian

4.1 The Rashba Hamiltonian and its order of magnitude

The spin-orbit coupling of an electron in an atom is known in atomic physics to give rise to splitting of the energy levels, part of the so-called fine structure [Sakurai, p.304-307]. A similar effect arises for the conduction electrons in a solid in an external electric field, i.e. spin-splitting the energy.

Consider a conduction electron moving in the x direction in a homogeneous electric field produced by a plate capacitor, see figure 8. We consider the Lorentz transformation of the electromagnetic field from the capacitors rest frame S to the electrons rest frame S' , which is moving with constant velocity v along the x direction relative to S . In S we have $\mathbf{E} = (0, E_y, 0)$, so the Lorentz transformation gives the following fields in the electrons rest frame S' :

$$\mathbf{E}' = (0, \gamma E_y, 0) \quad \mathbf{B}' = (0, 0, -\gamma \frac{v}{c^2} E_y)$$

where $\gamma = \frac{1}{\sqrt{1 - (\frac{v}{c})^2}}$ is to a very good approximation unity, because we do not work at relativistic velocities. The electrons “feel” the magnetic field \mathbf{B}' . We can now use the basic spin interaction Hamiltonian $\hat{H} = -\boldsymbol{\mu} \cdot \mathbf{B}$ with $\boldsymbol{\mu} = -\frac{g\mu_B}{2} \hat{\boldsymbol{\sigma}}$ to find the Hamiltonian for spin-orbit coupling:

$$\hat{H}_{s-o} = -\boldsymbol{\mu} \cdot \mathbf{B}' = -\frac{g\mu_B \gamma}{2c^2 m} E_y \hat{p}_x \hat{\sigma}_z$$

We can easily generalize this result to situations where $\mathbf{v} = (v_x, v_y, v_z)$ and $\mathbf{E} = \mathbf{E}(\mathbf{r}, t)$ and obtain $\hat{H}_{s-o} = -\frac{g\mu_B}{2c^2 m} (\hat{\mathbf{p}} \times \mathbf{E}) \cdot \hat{\boldsymbol{\sigma}}$, because at $\mathbf{B} = \mathbf{0}$ we can use the Lorentz transformation as $\mathbf{B}' = -\frac{\gamma}{c^2} (\mathbf{v} \times \mathbf{E})$ [Griffiths, p.532] and by inserting this into $\hat{H} = -\boldsymbol{\mu} \cdot \mathbf{B}'$, we get \hat{H}_{s-o} right away.

The order of magnitude of this effect at a realistic Fermi velocity $v = 10^6 \frac{m}{s}$ [Ashcroft & Mermin, p.36] and even for an extreme electric field $E = 10^{10} \frac{V}{m}$ is only $10^{-5} eV$. ($g_{\text{electron}} = 2$ and $\mu_B = \frac{e\hbar}{2m}$ were used). This is very small considered the extreme electric field, so spin-orbit coupling as a relativistic effect is actually not seen in normal solids!

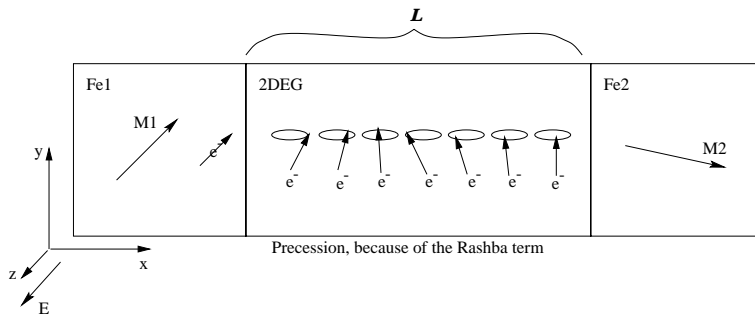


Figure 9: Geometry of the system

Nevertheless in a 2 dimensional electron gas (2DEG), which may exist in the (narrow) gap between two semiconductors, e.g. InAlAs and InGaAs, calculations of the band structure [de Silva] show an energy term similar to spin-orbit coupling:

$$\hat{H}_R = \alpha(\hat{\mathbf{p}} \times \mathbf{E}) \cdot \hat{\boldsymbol{\sigma}}$$

Here α is no longer $\frac{q\mu_B}{2c^2m}$. The expectation value of $\langle \alpha E \rangle$ times \hbar at realistic electric fields is of the order $10^{-11} eVm$ [Bauer]. By using the Fermi wave vector k_F of order $10^{10} m^{-1}$, H_R is of the order $10^{-1} eV$, i.e. 10^4 times greater than the relativistic effect. This Hamiltonian \hat{H}_R is called the Rashba Hamiltonian and was first considered in 1959 by É.I. Rashba [Rashba].

4.2 Application of H_R to a system with Fe-magnets and a 2DEG.

As an application of the Rashba effect, we consider a system consisting of a 2DEG with two semiconductor-ferromagnets as contacts in both ends (see figure 9). We would like to calculate the transmission for electrons through this system, hereby obtaining the conductance, as a function of the Rashba-parameter $\langle \alpha E \rangle$ and the magnetization in the two ferromagnets. Since $\langle \alpha E \rangle$ may be controlled to some extent by an external electric field, this is what is interesting for application in a real experimental setup.

Before we dwell on the calculations involved in this problem, we would like to give an overview of what is happening in a qualitative way. In the following we refer to figure 9. We consider an electron from the left ferromagnet through the 2DEG and into the right ferromagnet. In the left ferromagnet with magnetization \mathbf{M}_1 , the electrons spin are polarized in favor of the down direction, i.e. the direction anti-parallel with the magnetization. At the interface between the ferromagnet and the 2DEG, scattering of the electrons occurs in the following way: a fraction of the electrons are reflected with their spin unchanged, but also

a fraction (which, for our special problem, actually will turn out to be zero) will be reflected into the down state in the ferromagnet. Now, for the transmitted electrons there are also two possible (spin) states, namely up and down, but this time measured relative to the eigenstates of the Rashba-Hamiltonian, which are in general different from those in the ferromagnets. The eigenstates of the Rashba Hamiltonian suggest that one could speak of a pseudo magnetization (depending on \mathbf{k}) in the 2DEG. Therefore, as will be shown later, spin precession occurs for the transmitted electrons, and the spinor for a transmitted electron will change as the electron travels through the 2DEG. Reaching the right ferromagnet, again a certain fraction will be reflected into the two eigenstates in the 2DEG and a certain fraction will be transmitted into the two eigenstates in the second ferromagnet, according to what state the precessing electron is in and to what magnetization there is in this ferromagnet.

In 1990 [Datta & Das] proposed this system and that one should be able to control the current through the system by applying an external electric field, thereby controlling the Rashba-parameter and the precession, and controlling the current through the system by the means of only small changes in the external electric field.

4.3 Calculation of the transport properties

4.3.1 Eigenstates in the ferromagnets

We will now find the energy spin-splitting for the conduction electrons and the energy eigenstates in the ferromagnets.

We assume that the energy bands are quadratic in \mathbf{k} , so that the kinetic part of the Hamiltonian is $\hat{H}_0 = \frac{\hbar^2 \mathbf{k}^2}{2m_{\text{Fe}}^*}$, where m_{Fe}^* is the effective mass assumed to be isotropic in space.

The conduction electrons spin interact with the atoms in the ferromagnet via the exchange interaction, as in the spin filter section 3.1, so the Hamiltonian reads $\hat{H}_B = \Delta \frac{\mathbf{M}}{M} \cdot \hat{\boldsymbol{\sigma}}$, where $\mathbf{M} = M(\sin \theta \cos \phi, \sin \theta \sin \phi, \cos \theta)$ is the magnetization, and Δ is the material dependent exchange energy found experimentally. The Hamiltonian also consists of a constant term E_0^{Fe} which is the lowest subband energy in the ferromagnet. By calculating the inner product $\mathbf{M} \cdot \hat{\boldsymbol{\sigma}}$ one gets the total Hamiltonian as¹³:

$$\hat{H} = \hat{H}_0 + \hat{H}_B + E_0^{\text{Fe}} = \frac{\hbar^2 \mathbf{k}^2}{2m_{\text{Fe}}^*} \begin{pmatrix} 1 & 0 \\ 0 & 1 \end{pmatrix} + \Delta \begin{pmatrix} \cos \theta & \sin \theta e^{-i\phi} \\ \sin \theta e^{i\phi} & -\cos \theta \end{pmatrix} + E_0^{\text{Fe}} \begin{pmatrix} 1 & 0 \\ 0 & 1 \end{pmatrix}. \quad (28)$$

¹³Another way to find \hat{H}_B is to rotate σ_z so it becomes parallel with \mathbf{M} and then write $\hat{H}_B = \Delta \sigma_z^{\text{rot}}$ as done in [Bauer].

To find the eigenenergies and the energy eigenstates, we solve the time independent Schrödinger equation by diagonalizing the Hamiltonian (28). If θ is not 0 or π we find¹⁴:

$$E_{\pm}^{\text{Fe}} = E_0^{\text{Fe}} + \frac{\hbar^2 \mathbf{k}^2}{2m_{\text{Fe}}^*} \pm \Delta \quad \psi_{\pm}^{\text{Fe}}(x, y, z) = N_{\pm}^{\text{Fe}} e^{i\mathbf{k}\cdot\mathbf{r}} \begin{pmatrix} \cos \theta \pm 1 \\ \sin \theta e^{i\phi} \end{pmatrix} \quad (29)$$

as eigenenergies and eigenstates, where “+” and “−” represent up- and down states relative to the magnetization (see figure 10). Here N_{\pm}^{Fe} is the normalization, which we will return to later (in section 4.3.3). So there is an energy splitting of 2Δ of two conduction electrons with the same size of the wave vector $\mathbf{k} = (k_x, k_y, k_z)$ but different spin.

4.3.2 Eigenstates in the 2DEG

As in the ferromagnets we will find the energy and energy eigenstates in the 2DEG. Here the Rashba contribution is present, so by assuming quadratic energy bands again, we obtain the Hamiltonian as:

$$\hat{H} = \hat{H}_0 + \hat{H}_{\text{R}} = \frac{\hat{\mathbf{p}}^2}{2m_{\text{R}}^*} + \alpha(\hat{\mathbf{p}} \times \mathbf{E}) \cdot \hat{\boldsymbol{\sigma}} + E_0^{\text{R}} \begin{pmatrix} 1 & 0 \\ 0 & 1 \end{pmatrix}, \quad (30)$$

where E_0^{R} is the lowest subband energy in the 2DEG.

In the specific system, we consider the 2DEG to be in the xy -plane with a perpendicular electric field (see figure (9) on page 18), so $\hat{\mathbf{p}} = (\hat{p}_x, \hat{p}_y, 0)$ and $\mathbf{E} = (0, 0, E)$ which gives¹⁵:

$$\hat{H} = \begin{pmatrix} E_0^{\text{R}} + \frac{\hbar^2 \mathbf{k}^2}{2m_{\text{R}}^*} & \langle \alpha E \rangle \hbar (\hat{k}_y + i\hat{k}_x) \\ \langle \alpha E \rangle \hbar (\hat{k}_y - i\hat{k}_x) & E_0^{\text{R}} + \frac{\hbar^2 \mathbf{k}^2}{2m_{\text{R}}^*} \end{pmatrix} \quad (31)$$

by using $\hat{p}_i = \hbar \hat{k}_i$. As before we diagonalize \hat{H} to find the eigenenergies and eigenstates. When $k = \sqrt{k_x^2 + k_y^2} \neq 0$ we get¹⁶:

$$E_{\pm}^{\text{R}} = E_0^{\text{R}} + \frac{\hbar^2 (k_x^2 + k_y^2)}{2m_{\text{R}}^*} \pm \langle \alpha E \rangle \hbar \sqrt{k_x^2 + k_y^2} \quad (32)$$

$$\psi_{\pm}^{\text{R}}(x, y) = N_{\pm}^{\text{R}} e^{i(k_x x + k_y y)} \begin{pmatrix} \pm \frac{k_y + ik_x}{\sqrt{k_x^2 + k_y^2}} \\ 1 \end{pmatrix} \quad (33)$$

¹⁴If $\theta = 0$ or π , \hat{H} is already diagonal, so the eigenenergies are $E_{\pm}^{\text{Fe}} = E_0^{\text{Fe}} + \frac{\hbar^2 \mathbf{k}^2}{2m_{\text{Fe}}^*} \pm \Delta$ and the eigenstates is $\psi_+^{\text{Fe}} = N_+ e^{i\mathbf{k}\cdot\mathbf{r}} \begin{pmatrix} 1 \\ 0 \end{pmatrix}$ and $\psi_-^{\text{Fe}} = N_- e^{i\mathbf{k}\cdot\mathbf{r}} \begin{pmatrix} 0 \\ 1 \end{pmatrix}$, where N_{\pm} is the normalization constants.

¹⁵In [Bauer] there is a wrong sign here, which penetrates the calculations.

¹⁶If $k = 0$, the problem is obviously not interesting.

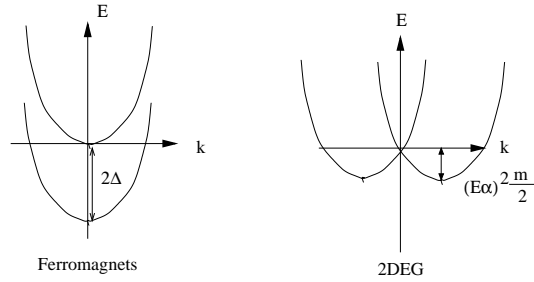


Figure 10: Energy bands in the two different materials

where N_{\pm}^R are the normalization constants to be determined later. E_{\pm}^R can also be written as

$$E_{\pm}^R = E_0^R + \frac{\hbar^2}{2m_R^*}((k \pm k_R)^2 - k_R^2) \quad (34)$$

by introducing $k_R = \frac{\alpha E m^*}{\hbar}$, which will be a convenient form later on. For the eigenstates, we see a very peculiar phenomenon, namely that the eigenstate is dependent on the direction of the wave vector $\mathbf{k} = (k_x, k_y, 0)$ and thereby on the direction the electron travels! Furthermore the energy splitting depends on the size $k = \sqrt{k_x^2 + k_y^2}$. This is in contrast to the ferromagnets (see equation (29)), where the energy splitting and the spin part of the eigenstates are independent of both the direction and size of \mathbf{k} . This difference arises, because $\hat{\mathbf{p}} \times \mathbf{E}$ can be seen as the effective B field the electron feels and it is dependent of both size and direction of $\hat{\mathbf{p}}$. In figure 10 we show the difference between the energy bands in the two materials.

4.3.3 Normalization of the eigenstates and derivation of the velocity operators.

There are different ways to normalize the eigenstates found in the previous sections. The most common is to require $\langle \psi | \psi \rangle = 1$, i.e. that the probability of finding the particle in some state is unity.

However, we choose to normalize in another manner. We are going to use the normalization, arising from letting the probability current $|\bar{\mathbb{J}}| = 1$. This is an often used condition in scattering problems ([Flensberg] and [Bauer]), because the transmission and reflection coefficients simply becomes the square of the absolute value of the amplitudes of the respective wavefunctions as we shall see later (section 4.3.5).

The probability current is found by imposing the condition from the continuity equation: $\frac{\partial \rho}{\partial t} = -\nabla \cdot \bar{\mathbb{J}}$, where ρ is the particle density. This is a statement of the conservation of matter. In the ferromagnets $\bar{\mathbb{J}}$ becomes the usual $\bar{\mathbb{J}} = \frac{\hbar}{2m_{\mp}^* i}(\psi^* \nabla \psi - \psi \nabla \psi^*)$ [Liboff, p.227]. In the 2DEG things are not so simple,

because the potential depends linearly on \hat{p} (cf. (30)). However, to keep things as simple as possible, we are going to consider only the one dimensional problem, and we will therefore normalize the eigenstates in the 2DEG in one dimension only. We do this by letting $\mathbb{J}_x = 1$.¹⁷ To derive \mathbb{J}_x in the 2DEG we identify ρ with $|\psi|^2$ and use the time dependent Schrödinger equation $\frac{\partial\psi}{\partial t} = -\frac{i}{\hbar}\hat{H}\psi$ and its complex conjugate $\frac{\partial\psi^*}{\partial t} = \frac{i}{\hbar}(\hat{H}\psi)^*$. By using the form of our Hamiltonian, $\hat{H}_R = \frac{\hat{p}_x^2}{2m_R^*} + A\hat{p}_x$, where we have temporarily defined $A = -\langle\alpha E\rangle\hat{\sigma}_y$, we find¹⁸:

$$\begin{aligned}\frac{\partial|\psi|^2}{\partial t} &= \frac{\partial(\psi^* \cdot \psi)}{\partial t} = \psi^* \frac{\partial\psi}{\partial t} + \frac{\partial\psi^*}{\partial t} \psi \\ &= \frac{i}{\hbar}(-\psi^* \hat{H}\psi + (\hat{H}\psi)^* \psi) \\ &= \frac{\hat{p}_x}{2i\hbar} \left(\psi^* \left(\frac{\hat{p}_x}{m_R^*} + A \right) \psi + \psi \left(\left(\frac{\hat{p}_x}{m_R^*} + A \right) \psi \right)^* \right)\end{aligned}\quad (35)$$

By comparing with the continuity equation we get¹⁹

$$\mathbb{J}_x = \frac{1}{2} \left\{ \psi^* \left(\frac{\hat{p}_x}{m_R^*} - \langle\alpha E\rangle\hat{\sigma}_y \right) \psi + \psi \left(\left(\frac{\hat{p}_x}{m_R^*} - \langle\alpha E\rangle\hat{\sigma}_y \right) \psi \right)^* \right\}.\quad (36)$$

By introducing the velocity operator \hat{v}_x we will see that this expression has a simple interpretation because we will find that we may write

$$\mathbb{J}_x = \frac{1}{2}(\psi^* \hat{v}_x \psi + \psi (\hat{v}_x \psi)^*).\quad (37)$$

The way we introduce the velocity operators is by considering the classical Hamiltonian's equations of motion [Goldstein, p.342] and simply replacing the classical Hamiltonian with the Hamilton operator, obtaining $\hat{v}_x = \frac{\partial\hat{H}}{\partial\hat{p}_x}$ [Bauer].²⁰ In the ferromagnets and in the 2DEG the velocity operators are:

$$\hat{v}_x^{\text{Fe}} = \frac{\partial(\hat{H}_0 + \hat{H}_B)}{\partial\hat{p}_x} = \frac{\hat{p}_x}{m_{\text{Fe}}^*} \begin{pmatrix} 1 & 0 \\ 0 & 1 \end{pmatrix}\quad (38)$$

$$\hat{v}_x^{\text{R}} = \frac{\partial(\hat{H}_0 + \hat{H}_R)}{\partial\hat{p}_x} = \begin{pmatrix} \frac{\hat{p}_x}{m_R^*} & i\langle\alpha E\rangle \\ -i\langle\alpha E\rangle & \frac{\hat{p}_x}{m_R^*} \end{pmatrix}\quad (39)$$

It is seen that in the ferromagnets \hat{v}_x^{Fe} is exactly $\frac{\hat{p}_x}{m_{\text{Fe}}^*}$ as one expects, but in the 2DEG the \hat{p}_x dependence in the Rashba term makes \hat{v}_x^{R} more complicated²¹. By

¹⁷Actually we consider the wave function for the electron to be a product of a plane wave in the x -direction and a standing wave with only one mode in the y -direction so there will be no net current in the y -direction.

¹⁸The complete calculations are shown in appendix B

¹⁹Up to an additive constant.

²⁰This is also a natural way of turning the group velocity [Kittel, p.102] $\hat{v}_g = \frac{1}{\hbar} \frac{\partial E}{\partial k}$ into an operator.

²¹This fact was disregarded by [Grundler] and corrected recently by [Bauer].

comparing (38) and (39) with (36) we obtain (37) which states that \mathbb{J}_x is just the real part of $\psi^* \hat{v}_x^R \psi$, which is intuitively appealing.

Finally the normalization constants are found:

$$\mathbb{J}_x^{\text{Fe}} = 1 \Rightarrow N_{\pm}^{\text{Fe}} = \sqrt{\frac{m_{\text{Fe}}^*}{\hbar k_x} \frac{1}{2(1 \pm \cos \theta)}} \quad (40)$$

and:

$$\mathbb{J}_x^{\text{R}} = 1 \Rightarrow N_{\pm}^{\text{R}} = \sqrt{\frac{m_{\text{R}}^*}{2\hbar k_x \left(1 \pm \frac{k_{\text{R}}}{k_x}\right)}} \quad (41)$$

where $k_{\text{R}} = \frac{\langle \alpha E \rangle m_{\text{R}}^*}{\hbar}$. If $\theta = 0, \pi$, N_{\pm}^{Fe} does not make sense, but that is no problem because our eigenstates were not valid for these values. As we will see later $N_+^{\text{R}} = N_-^{\text{R}}$ in our problem, because of energy conservation.

4.3.4 Energy considerations and wave vectors

We are going to calculate the wave vectors for the different electron states under the assumption that the states have the same energy. In our model for the ferromagnets the eigenenergies are given by (29). Choosing $E_0^{\text{Fe}} = -\Delta$ makes the spin-up electrons have zero potential energy, so that a spin-up electron with Fermi energy, E_F will have wave vector $k_{\uparrow} = \sqrt{\frac{2m_{\text{Fe}}^* E_F}{\hbar^2}}$. From the equation $-\Delta + \frac{\hbar^2 k_{\downarrow}^2}{2m_{\text{Fe}}^*} - \Delta = E_F$ for the spin-down electrons at the Fermi energy, we infer that they will have wave vectors $k_{\downarrow} = \sqrt{\frac{2m_{\text{Fe}}^* (E_F + 2\Delta)}{\hbar^2}}$, where we have taken the positive solution.

The energy splitting 2Δ can be found as a function of the Fermi energy E_F by using the knowledge of the fraction $\frac{N_{\downarrow}}{N}$ which is the fraction of conduction electrons in the ferromagnet with spin down. For iron and nickel this fraction is 0.6 and 0.9 [Prinz]. By using the fact that the electrons travel with the Fermi energy we get:

$$\begin{aligned} E_F &= E_+^{\text{Fe}} = \frac{\hbar^2 \mathbf{k}_{\uparrow}^2}{2m_{\text{Fe}}^*} \\ &= E_-^{\text{Fe}} = \frac{\hbar^2 \mathbf{k}_{\downarrow}^2}{2m_{\text{Fe}}^*} - 2\Delta \end{aligned}$$

Where $E_{\text{kin},-}^{\text{Fe}} = \frac{\hbar^2 \mathbf{k}_{\downarrow}^2}{2m_{\text{Fe}}^*}$ is the kinetic energy for spin down and $E_{\text{kin},+}^{\text{Fe}} = E_F$. Now as $N_{\uparrow}(N_{\downarrow})$ is proportional to $k_{\uparrow}^3(k_{\downarrow}^3)$ [Kittel, p.146-149]²² we have:

²²Kittel's argument for this proportionality has to be modified a bit to fit our situation, but it is still true.

$$\frac{N_{\uparrow}}{N_{\downarrow}} = \frac{k_{\uparrow}^3}{k_{\downarrow}^3} \quad \frac{E_{kin,+}^{\text{Fe}}}{E_{kin,-}^{\text{Fe}}} = \frac{k_{\uparrow}^2}{k_{\downarrow}^2} \quad E_{kin,-}^{\text{Fe}} - E_{kin,+}^{\text{Fe}} = 2\Delta$$

which gives:

$$\Delta = \frac{1}{2} \left(\left(\frac{N_{\downarrow}}{N_{\uparrow}} \right)^{\frac{2}{3}} - 1 \right) E_F$$

In iron, E_F is 11eV [Ashcroft & Mermin, p.38], so Δ is 1.65eV.

Now $k_{\uparrow} = \sqrt{\frac{2m_{\text{Fe}}^* E_F}{\hbar^2}}$ and $k_{\downarrow} = \sqrt{\frac{2m_{\text{Fe}}^*(E_F+2\Delta)}{\hbar^2}}$, where we have taken the positive solutions.

In the Rashba-split 2DEG we have the eigenenergies given by (34) on page 21. Choosing $E_0^{\text{R}} = 0$ gives the size of the wave vectors for an electron at the Fermi energy:

$$k_{\pm} = \mp k_R + \sqrt{k_R^2 + k_F^2} \quad (42)$$

according to what spin-state it is in. Remember $k_R = \langle \alpha E_z \rangle m / \hbar$. We have chosen the positive solution for the wave vectors k_{\pm} . Because the pseudo magnetization and thereby the Rashba-energy depends on what direction the electron moves, also the wave vector depends on the travel direction in the same spin state.

In one dimension equation (42) shows that $N_{+}^{\text{R}} = N_{-}^{\text{R}}$, because $k_{\pm} \pm k_R = +\sqrt{k_R^2 + k_F^2}$, so

$$N_{\pm}^{\text{R}} = \sqrt{\frac{m_{\text{R}}^*}{2\hbar \sqrt{k_R^2 + k_F^2}}}. \quad (43)$$

From now on we consider only the one-dimensional problem, where the transport is along the x -axis (see figure 9 on page 18). From (41) it is seen that the normalization in the one-dimensional case is the same for the two spin-states. For an electron traveling in the $+x$ -direction in the “+” spin-state, (\uparrow) , the wave vector is k_{+} . If the electron in the same spin state is moving in the $-x$ -direction, the wave vector is k_{-} , because the pseudo-magnetization changes sign, when the electron travels in the opposite direction.

4.3.5 Transmission and reflection at the interfaces

We are now ready to calculate the total wavefunction in the system, by using the solutions to the Schrödinger equation in the different regions. By imposing continuity conditions, we will be able to find reflection and transmission coefficients at the interfaces as functions of the parameters in the problem, especially the magnetizations directions and the “strength” of the Rashba effect, $\langle \alpha E \rangle$.

In the first (left) ferromagnet the wavefunction will consist of a superposition of three plane waves, namely

$$\psi^{\text{Fe}_1} = \underbrace{N_{\uparrow}^{\text{Fe}_1} e^{ik_{\uparrow}x} \begin{pmatrix} \cos \theta_1 + 1 \\ \sin \theta_1 e^{i\varphi_1} \end{pmatrix}}_{\text{Incoming}} + \underbrace{r_{1\uparrow} N_{\uparrow}^{\text{Fe}_1} e^{-ik_{\uparrow}x} \begin{pmatrix} \cos \theta_1 + 1 \\ \sin \theta_1 e^{i\varphi_1} \end{pmatrix}}_{\text{up-reflected}} + \underbrace{r_{1\downarrow} N_{\downarrow}^{\text{Fe}_1} e^{-ik_{\downarrow}x} \begin{pmatrix} \cos \theta_1 - 1 \\ \sin \theta_1 e^{i\varphi_1} \end{pmatrix}}_{\text{down-reflected}} \quad (44)$$

because the reflected electron will in general have a possibility to undergo a spin-flip, thereby being reflected into the down-state. In the 2DEG there will be transmitted states from the left ferromagnet and reflected states from the second interface. In the 2DEG we therefore have the wavefunction

$$\psi^{\text{R}} = N^{\text{R}} \left(\underbrace{t_{1\uparrow} e^{ik_{\uparrow}x} \begin{pmatrix} i \\ 1 \end{pmatrix}}_{\text{transmitted-“up”}} + \underbrace{t_{1\downarrow} e^{ik_{\downarrow}x} \begin{pmatrix} -i \\ 1 \end{pmatrix}}_{\text{transmitted-“down”}} + \underbrace{r_{2\uparrow} e^{-ik_{\uparrow}x} \begin{pmatrix} i \\ 1 \end{pmatrix}}_{\text{reflected-“up”}} + \underbrace{r_{2\downarrow} e^{-ik_{\downarrow}x} \begin{pmatrix} -i \\ 1 \end{pmatrix}}_{\text{reflected-“down”}} \right). \quad (45)$$

In the second ferromagnet, there will be only waves traveling in the $+x$ -direction because we imagine making a perfect measurement of the transmission in this ferromagnet, thereby having no reflected states in this region. The wavefunction is

$$\psi^{\text{Fe}_2} = \underbrace{t_{2\uparrow} N_{\uparrow}^{\text{Fe}_2} e^{ik_{\uparrow}x} \begin{pmatrix} \cos \theta_2 + 1 \\ \sin \theta_2 e^{i\varphi_2} \end{pmatrix}}_{\text{up-transmitted}} + \underbrace{t_{2\downarrow} N_{\downarrow}^{\text{Fe}_2} e^{ik_{\downarrow}x} \begin{pmatrix} \cos \theta_2 - 1 \\ \sin \theta_2 e^{i\varphi_2} \end{pmatrix}}_{\text{down-transmitted}} \quad (46)$$

To find the various coefficients ($r_{1,2,\uparrow\downarrow}, t_{1,2,\uparrow\downarrow}$), we impose continuity conditions at the interfaces. First, the wavefunction has to be continuous, according to the general quantum mechanical interpretation of the wavefunction as a measure of probability. Imposing this criterion at the interfaces $x = 0$ and $x = L$, we get

$$\psi^{\text{Fe}_1}(0) = \psi^{\text{R}}(0) \quad \text{and} \quad \psi^{\text{R}}(L) = \psi^{\text{Fe}_2}(L) \quad (47)$$

Secondly, expressing mathematically that the number of electrons is conserved locally, the probability flux has to be continuous, which in more simple scattering problems, where the velocity operator is simply proportional to the gradient operator ∇ , reduces to the condition that the derivative of the wavefunction be continuous. But in our problem, where the velocity operator is *not* simply proportional to the gradient operator, this is not the case. The flux continuity condition is therefore:

$$\hat{v}_x^{\text{Fe}_1} \psi^{\text{Fe}_1} |_{x=0} = \hat{v}_x^{\text{R}} \psi^{\text{R}} |_{x=0} \quad \text{and} \quad \hat{v}_x^{\text{R}} \psi^{\text{R}} |_{x=L} = \hat{v}_x^{\text{Fe}_2} \psi^{\text{Fe}_2} |_{x=L} \quad (48)$$

with the velocity operators given by (38) and (39) on page 22.

Performing these operations gives a system of 8 linear equations with 8 unknowns²³, which is solved with the help of *Mathematica*. The result, the 8 coefficients $r_{1,2\uparrow\downarrow}, t_{1,2\uparrow\downarrow}$ are actually almost the reflection and transmission coefficients, as defined for example in [Liboff, p.227], i.e. they are themselves a measure for the transmitted and reflected probability current density, which is seen as follows. The transmission and reflection coefficients are defined as

$$T = \left| \frac{\mathbb{J}_{\text{trans}}}{\mathbb{J}_{\text{inc}}} \right| \quad \text{and} \quad R = \left| \frac{\mathbb{J}_{\text{refl}}}{\mathbb{J}_{\text{inc}}} \right| \quad (49)$$

with incoming, transmitted and reflected states in one dimension. But with

$$\mathbb{J}_x = \frac{1}{2}(\psi^* \hat{v}_x \psi + \psi(\hat{v}_x \psi)^*) \quad (50)$$

the current for e.g. $t_{2\uparrow} N^{\text{Fe}\uparrow} e^{ik_{\uparrow}x} \begin{pmatrix} \cos(\theta_2)+1 \\ \sin(\theta_2)e^{i\varphi_2} \end{pmatrix}$ is $|t_{2\uparrow}|^2$ because of the chosen normalization.²⁴ This allows us to identify $T_{2\uparrow} = |t_{2\uparrow}|^2$, for the up-transmission coefficient through the system, and similarly for the other coefficients.

4.3.6 Precession in the 2DEG

We now show, that in the 2DEG, the transmitted electrons precess as a function of x , due to the difference in wave vector for the two different spin-eigenstates. We project the state in the 2DEG onto the eigenstates in the second ferromagnet as²⁵:

$$\psi^{\text{R}} = \langle \psi_+^{\text{Fe}_2} | \psi^{\text{R}} \rangle \psi_+^{\text{Fe}_2} + \langle \psi_-^{\text{Fe}_2} | \psi^{\text{R}} \rangle \psi_-^{\text{Fe}_2} \quad (51)$$

A plot²⁶ of the squared amplitudes for the two coefficients as a function of x , is seen in figure 11, where the precession is clear. Noteworthy, the precession is on realistic²⁷ length scales, with a realistic value for $\langle \alpha E \rangle$.

We see that the probability of finding the down state is always the larger. This can be understood in terms of what direction in space the electron is precessing about. An intuitive picture of the situation is that the amount of transmission at L is determined by how much the electron has precessed in traveling through the 2DEG. By comparing figure 11 to figure 13(c) we see that there is a resemblance, which supports the intuitive understanding of the problem.

²³Actually, it can be shown that $r_{1\downarrow} = 0$, using that the group velocities for the two spin states in the 2DEG are the same, which is only correct in one dimension.

²⁴Which is seen by a straightforward but tedious calculation.

²⁵To be able to do this we must change the normalization of the wavefunctions to the one obtained from imposing $\langle \psi | \psi \rangle = 1$, which is done for this section only.

²⁶This plot is for a one interface problem, only.

²⁷Which will be made precise later.

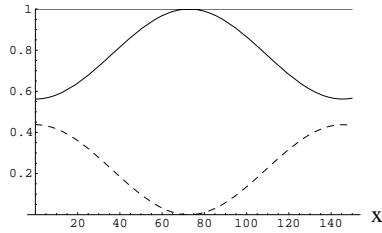


Figure 11: Probability for the precessing state in the 2DEG to be in the up-state(---) and the down-state(—) in the right ferromagnet and the sum, as a function of x measured in nm . The plot is for the same effective mass, $0.15m_e$ in the two materials and for a realistic value of $\langle\alpha E\rangle$.

4.4 The conductance of the system.

The calculations so far has not included a chemical potential difference between the two contacts. So we have at the present state no net current through the system. But by introducing a small bias (compared to the order of the energy splitting 2Δ) we can still as a first approximation [Egues, p.4580] use our calculations in the zero-bias situation.

The conductance of the system is given by the Landauer-Büttiker formula [Flensberg, p.7], which we will not show, as:

$$G = \frac{e^2}{h} \sum T_n \quad (52)$$

where the sum is over all possible ways that an electron can be transmitted through the 2DEG and T_n is the transmission coefficients. To find all transmission possibilities we have to consider both incoming electrons with spin up and spin down. The spin up case is already treated and the spin down case is done similarly by sending $\psi_{in}^{Fe_1} = N_-^{Fe_1} e^{ik_{\downarrow}x} \begin{pmatrix} \cos\theta_1 - 1 \\ \sin\theta_1 e^{i\varphi_1} \end{pmatrix}$ into the 2DEG. So in all we have:

$$G = \frac{e^2}{h} ((T_{\uparrow\uparrow} + T_{\uparrow\downarrow}) + (T_{\downarrow\downarrow} + T_{\downarrow\uparrow})) \quad (53)$$

Where $T_{\uparrow\uparrow} = |t_{2\uparrow}|^2$ is the transmission coefficient for an incoming up-spin which transmits to the up state and $T_{\uparrow\downarrow} = |t_{2\downarrow}|^2$ is the transmission for an incoming up and transmitted down electron.

By using this formula we are in a position to find the conductance G as a function of $\langle\alpha E\rangle$, L and the two magnetization directions.

4.5 Results and comments

In figure 12 we plot the conductance (the constant line) as a function of the angles of the magnetizations together with the four transmission coefficients

$(T_{\uparrow\uparrow}, T_{\uparrow\downarrow}, T_{\downarrow\uparrow}, T_{\downarrow\downarrow})$, where the first subscript refers to the incoming state and the second to the transmitted state. It is seen that for all plots, $T_{\uparrow\uparrow}$ and $T_{\downarrow\downarrow}$ are not exactly equal, while $T_{\uparrow\downarrow}$ and $T_{\downarrow\uparrow}$ are the same. The conductance remains in all plots in figure 12 constant, the value depending on the other parameters, most dramatic on the difference of the effective masses. These plots are for $m_{\text{Fe}}^* = 0.23m_e$ and $m_{\text{R}}^* = 0.07m_e$ and in each plot, the non-varying angles are chosen randomly because numerical experiments show that these angles do not influence considerably on the conductance. So, for the conductance of the system, the angles are rather irrelevant, only influencing on whether the electrons have to turn their spin-direction before entering the second ferromagnet or not.

In figure 13(a) we show the conductance in units of $\frac{e^2}{h}$ of the system as a function of $\langle\alpha E\rangle$ for different effective masses for the ferromagnets and the constant value $m_{\text{R}}^* = 0.07m_e$ in the 2DEG. From the bottom to the top the effective mass is $m_{\text{Fe}}^* = 1\}\{0.81\}\{0.62\}\{0.23\}\{0.07$. It is seen that for $\langle\alpha E\rangle$ between 0 and $2 \cdot 10^4 \frac{m}{s}$, which is the realistic interval for the value for $\langle\alpha E\rangle$ [Bauer], the conductance is constant, i.e. we cannot make a transistor with changes the conductance by varying $\langle\alpha E\rangle$ on a realistic scale.

However, in figure 13(b) we show the conductance in units of $\frac{e^2}{h}$ for only one set of effective masses ($m_{\text{R}}^* = 0.07m_e$ and $m_{\text{Fe}}^* = 0.23m_e$), and it is seen, that one can control the conductance if $\langle\alpha E\rangle$ is allowed to be in the interval $0-150 \cdot 10^4 \frac{m}{s}$. These two results are in fact reasonable if we compare the size of $\langle\alpha E\rangle$ with another velocity in the system, namely the Fermi-velocity, which is of the order of $10^6 \frac{m}{s}$. So only when $\langle\alpha E\rangle$ approaches $10^6 \frac{m}{s}$ it becomes appreciable compared to v_F and the Rashba effect can be seen in the conductance.

In figure 13(c) we show that even if the conductance of the system is constant for realistic values of $\langle\alpha E\rangle$ the transmission coefficients may vary. The plot shows that for an incoming spin-down beam, the transmission to the two states in the second ferromagnet varies as a function of $\langle\alpha E\rangle$, even at realistic values. This reflects that the electrons are precessing in the 2DEG as described in section 4.3.6.

In figure 13(d) we try to model the system that is proposed in [Datta & Das],²⁸

²⁸Which cannot be done completely with our model, so the result may not be exact. However, we believe that at least the qualitative behaviour is representative

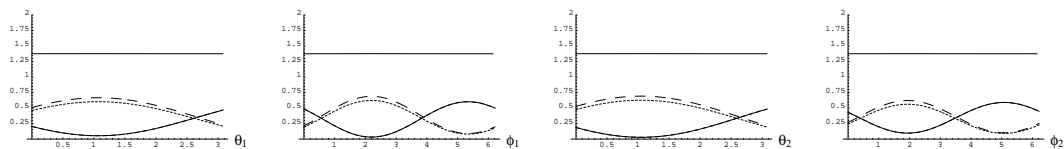


Figure 12: Plots of the conductance (constant) in units of $\frac{e^2}{h}$ and $T_{\uparrow\uparrow}(\dots), T_{\downarrow\downarrow}(- -), T_{\uparrow\downarrow}$ and $T_{\downarrow\uparrow}$, both (—) as functions of the angles of the magnetizations.

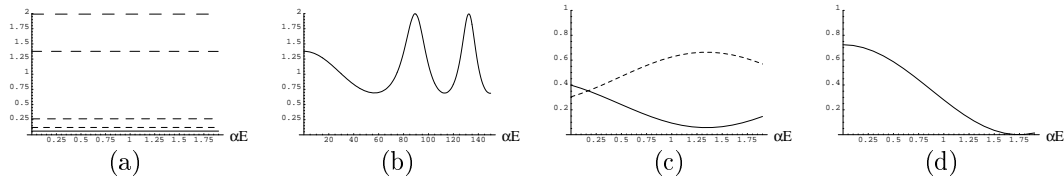


Figure 13: The dimension of $\langle \alpha E \rangle$ is in all plots $10^4 \frac{m}{s}$ ($2 \cdot 10^4 \frac{m}{s}$ corresponds to $\hbar \langle \alpha E \rangle = 10^{-11} eVm$) (a): Conductance of the system for different effective masses. (b): Conductance of the system for unrealistic large values of $\langle \alpha E \rangle$. (c): $T_{\downarrow\uparrow}$ (---) and $T_{\downarrow\downarrow}$ (—) (d): Conductance for a totally polarized ferromagnet as used in [Datta & Das]. All conductances are measured in units of $\frac{e^2}{h}$.

where total polarization of the electrons in the first and second ferromagnet (that is $\frac{N_{\downarrow}}{N_{\uparrow} + N_{\downarrow}} = 1$) is assumed. We send in only spin-down electrons and plot $T_{\downarrow\downarrow}$ which is in this situation equal to the conductance in units of $\frac{e^2}{h}$, because we assumed that only the favored state in the ferromagnet exists. This plot is made with both magnetizations in the $+x$ -direction. We conclude that if the polarization is complete in the ferromagnets, the conductance can be controlled at realistic scales for $\langle \alpha E \rangle$. But as seen in figure 13(a), the actual situation in a ferromagnet, with only partial polarization, leads to constant conductance.

At this point it must be pointed out that to make our considerations more realistic, the two dimensional problem should be considered. In this situation one would expect smaller effects, as pointed out in [Datta & Das].

4.6 A possible spin polarizer?

The spin free path in a ferromagnet is very small, because of the coupling of the spin to the magnetization, so even if we have a spin polarized current at the second interface ($x = L$), it is destroyed right away in the ferromagnet. So the considered system is not a possible spin polarizer.

This motivates us to replace the second ferromagnet with a non-magnetic semiconductor contact in which the spin free path is longer and can actually be enlarged by several orders of magnitude by doping the semiconductor [Fabian]. By the choice of materials it is possible to obtain the same effective mass m_{Fe}^* in the two contacts, but they will generally be different from m_{R}^* in the 2DEG. Now we apply a small external bias as before.

We assume that the eigenstates in the semiconductor are $\psi_{\uparrow}^s = N e^{ikx} \begin{pmatrix} 1 \\ 0 \end{pmatrix}$ and $\psi_{\downarrow}^s = N e^{ikx} \begin{pmatrix} 0 \\ 1 \end{pmatrix}$ with the same eigenenergy $E = \frac{\hbar^2 k^2}{2m^*}$ and $N = \sqrt{\frac{m^*}{\hbar k}}$, both spin independent.

The injected current can have different spin polarizations. In iron the fraction $\frac{N_{\downarrow}}{N_{\uparrow} + N_{\downarrow}}$ of conduction electrons with spin down is 0.6 and in nickel 0.9 [Prinz, p.58].

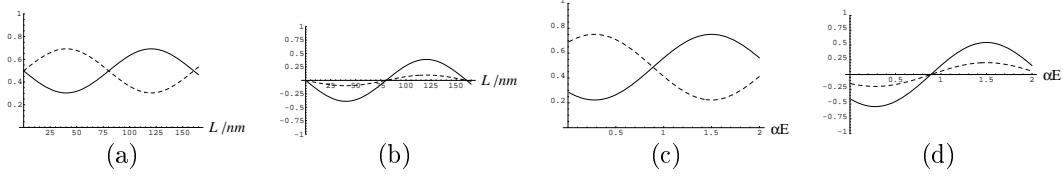


Figure 14: (a): T_{\uparrow} (—) and T_{\downarrow} (- -) as a function of L . (b): $\frac{T_{\uparrow}-T_{\downarrow}}{T_{\uparrow}+T_{\downarrow}}$ as a function of L , where $E_F = 10eV$, $\hbar\langle\alpha E\rangle = 10^{-11}eVm$, $\varphi = \frac{\pi}{3}$, $\theta = \frac{\pi}{2}$ and $m_R^* = 0.15m_e$ and $m_{Fe}^* = 0.25m_e$ were used in both (a) and (b). (c): T_{\uparrow} (—), T_{\downarrow} (- -) as a function of $\langle\alpha E\rangle \cdot 10^4 \frac{m}{s}$. Note that $\hbar\langle\alpha E\rangle = 10^{-11}eVm$, which is the realistic value, corresponds to $\langle\alpha E\rangle = 2 * 10^4 \frac{m}{s}$. (d): $\frac{T_{\uparrow}-T_{\downarrow}}{T_{\uparrow}+T_{\downarrow}}$ as a function of $\langle\alpha E\rangle \cdot 10^4 \frac{m}{s}$, where in (c) and (d) $L = 100nm$ and the rest as in (a) and (b).

Based on arguments involving the density operator [Sakurai, p.174-187] we get the transmission to the up state (\uparrow) T_{\uparrow} to be:

$$T_{\uparrow} = \frac{N_{\uparrow}}{N_{\uparrow} + N_{\downarrow}} |t_{2\uparrow}|^2 + \frac{N_{\downarrow}}{N_{\uparrow} + N_{\downarrow}} |t_{2\downarrow}|^2$$

where $t_{2\uparrow}$ and $t_{2\downarrow}$ is calculated for an incoming spin up. A similar equation for T_{\downarrow} is true.

In figure (14) we plot T_{\uparrow} , T_{\downarrow} and $\frac{T_{\uparrow}-T_{\downarrow}}{T_{\uparrow}+T_{\downarrow}}$ as a function of $\langle\alpha E\rangle$ and L , where $\frac{T_{\uparrow}-T_{\downarrow}}{T_{\uparrow}+T_{\downarrow}}$ is used as a measure for the polarization. For the $\frac{T_{\uparrow}-T_{\downarrow}}{T_{\uparrow}+T_{\downarrow}}$ plots, (—) corresponds to an incoming polarization $\frac{N_{\downarrow}}{N_{\uparrow}+N_{\downarrow}} = 0.9$ and (- -) to $\frac{N_{\downarrow}}{N_{\uparrow}+N_{\downarrow}} = 0.6$. We have taken $\frac{N_{\downarrow}}{N_{\uparrow}+N_{\downarrow}}$ for iron and nickel as representative values, even though we have a semiconductor ferromagnet. We see that the maximum size of the polarization is very sensitive to the incoming polarization. Furthermore since it is possible to control $\langle\alpha E\rangle$ by the external electric field to some extent, it is also possible to control the spin polarization from -0.6 to 0.6 (for $\frac{N_{\downarrow}}{N_{\uparrow}+N_{\downarrow}} = 0.9$) by changing the field. Numerical experiments show that the larger the incoming polarization, the larger the effect. As a function of L we can read off a suitable value for the length of the 2DEG region, if we wish to make a device with a specific polarization. By numerical experiments we found that changes in the magnetization direction does not change the showed graphs considerably so arbitrary values of θ and φ were chosen. So, we have in theory made a possible spin-polarizer, but not a spinfilter as in [Egues].

4.7 Conclusion

We have described the Rashba Hamiltonian for electrons in a 2DEG and considered a system consisting of a 2DEG with ferromagnetic contacts. In one dimension we have calculated transmission coefficients and shown that with realistic values for $\langle\alpha E\rangle$ the conductance is constant. However, precession in the 2DEG accounts for different transmission coefficients for the up- and down states in the second ferromagnet as a function of $\langle\alpha E\rangle$ - even at realistic values. At very large values for $\langle\alpha E\rangle$, the conductance shows oscillatory behaviour. If the system should be able to act as a transistor, as proposed by [Datta & Das], a fully polarized incoming beam is required, which is not realistic with normal ferromagnets. (One could therefore consider an incoming beam from a spin filter like the one we have described).

We have constructed a possible spin polarizer by substituting the second ferromagnet with a non-magnetic semiconductor. The spin-polarizer changes the polarization as a function of $\langle\alpha E\rangle$ and L . The polarization effect is very dependent on how much the initial beam is polarized - the effect increasing with the polarization.

From our point of view the most interesting question at the moment is to what extent $\langle\alpha E\rangle$ can be controlled.

References

- [Ashcroft & Mermin] Ashcroft, Neil W. and Mermin, N. David: Solid State Physics, College ed., Harcourt College Publishers 1976
- [Barnas] Camley,R.E. and Barnas,J.: Theory of Giant Magnetoresistance Effects in Magnetic Layered Structures with Antiferromagnetic Coupling, Phys. Rev. Lett., 63, no. 6, 7. Aug. 1989
- [de Vries] de Vries, J.W.C.: Interface scattering in triple layered polycrystalline thin Au|X|Au films (X=Fe,Co,Ni), Solid State Comm., Vol.65,No.3,pp.201-204,1988
- [Kittel] Kittel, Charles: Introduction to Solid State Physics, 7.ed., John Wiley & Sons 1996
- [Sakurai] Sakurai, J.J.: Modern Quantum Mechanics, Rev. Ed., Addison-Wesley 1994
- [Prinz] Prinz, Gary A.: Spin-Polarized Transport, Phys. Today, **48**,4,58 (1995)
- [IBM] www.storage.ibm.com/hardsoft/diskdrdl/technolo/gmr/gmr.htm
- [Egues] Egues, J. Carlos, Phys. Rev. Lett. **80**, 20, p.4578, 18 May 1998
- [Griffiths] Griffiths, David J.: Introduction to electrodynamics, 3rd ed., Prentice Hall 1999
- [Liboff] Liboff, Richard L.: Introductory Quantum Mechanics, Third edition, Addison Wesley 1998
- [Datta & Das] Datta, Supriyo and das, Diswajit: Electronic analog of the electro-optic modulator, Appl. Phys. Lett. **56** (7), Feb. 1990.
- [Rashba] Rashba, É.I.:Properties of semiconductors with an extremum loop, Sov.Phys. Solid State **2**, 1109 (1960)
- [Bauer] Molenkamp, Laurens W., Schmidt, Georg and Bauer, Gerrit E.W.: The Rashba Hamiltonian and electron transport, preprint from cond-mat/0104109, 6th April 2001.
- [de Silva] de Silva,E.A. Andrada, La Rocca,G.C. and Bassani,F.: Spin-orbit splitting of electronic states in semiconductor asymmetric quantum wells, Phys. Rev. B. vol.55, 24.
- [Flensberg] Flensberg, Karsten: Lecture notes on transport properties of mesoscopic systems, NBIfAFG, Ørsted Laboratory, 2000

- [Grundler] Grundler, D. :Phys. Rev. Lett. **86**,1058 (2001)
- [Goldstein] Goldstein, Herbert: Classical mechanics, 2.nd ed., Addison-Wesley 1980
- [Das] Das Sarma, S., Fabian, Jaroslav, Hu, Xuedong and Žutić, Igor: Spintronics: electron spin coherence, entanglement, and transport. cond-mat/9912040 v3 7 Mar 2000.
- [Hu] Das Sarma, S., Fabian, Jaroslav, Hu, Xuedong and Žutić, Igor: Theoretical Perspectives on Spintronics and Spin-Polarized Transport (Not published)
- [Fabian] Fabian, J. and Das Sarma, S.: Spin Relaxation of Conduction Electrons, cond-mat/9901170 18 Jan 1999

Appendix A

The g -function's coefficients

Now follows all the coefficients for the various g -functions. As is seen, the symmetry of the system manifests itself in these coefficients.

$$\begin{aligned}
A_{+\uparrow} &= -\exp\left(\frac{-b}{\tau |v_z|}\right) \\
A_{+\downarrow} &= -\exp\left(\frac{-b}{\tau |v_z|}\right) \\
A_{-\uparrow} &= \left[\left(1 + B_{\uparrow} \exp\left(\frac{-a}{\tau |v_z|}\right)\right) (1 - \mathcal{D}_{\uparrow}) - 1 \right] \exp\left(\frac{a}{\tau |v_z|}\right) \\
A_{-\downarrow} &= \left[\left(1 + B_{\downarrow} \exp\left(\frac{-a}{\tau |v_z|}\right)\right) (1 - \mathcal{D}_{\downarrow}) - 1 \right] \exp\left(\frac{a}{\tau |v_z|}\right) \\
B_{+\uparrow} &= \left[\left(1 - \exp\left(\frac{a-b}{\tau |v_z|}\right)\right) (1 - \mathcal{D}_{\uparrow}) - 1 \right] \exp\left(\frac{-a}{\tau |v_z|}\right) \\
B_{+\downarrow} &= \left[\left(1 - \exp\left(\frac{a-b}{\tau |v_z|}\right)\right) (1 - \mathcal{D}_{\downarrow}) - 1 \right] \exp\left(\frac{-a}{\tau |v_z|}\right) \\
B_{-\uparrow} &= T_{\uparrow\uparrow}(1 + C_{-\uparrow}) + T_{\uparrow\downarrow}(C_{-\downarrow} + 1) - 1 \\
B_{-\downarrow} &= T_{\downarrow\downarrow}(1 + C_{-\downarrow}) + T_{\downarrow\uparrow}(C_{-\uparrow} + 1) - 1 \\
C_{+\uparrow} &= T_{\uparrow\uparrow}(1 + B_{+\uparrow}) + T_{\uparrow\downarrow}(1 + B_{+\downarrow}) - 1 \\
C_{+\downarrow} &= T_{\downarrow\downarrow}(1 + B_{+\downarrow}) + T_{\downarrow\uparrow}(1 + B_{+\uparrow}) - 1 \\
C_{-\uparrow} &= \left[\left(1 - \exp\left(\frac{a-b}{\tau |v_z|}\right)\right) (1 - \mathcal{D}_{\uparrow}) - 1 \right] \exp\left(\frac{-a}{\tau |v_z|}\right) \\
C_{-\downarrow} &= \left[\left(1 - \exp\left(\frac{a-b}{\tau |v_z|}\right)\right) (1 - \mathcal{D}_{\downarrow}) - 1 \right] \exp\left(\frac{-a}{\tau |v_z|}\right) \\
D_{+\uparrow} &= \left[\left(1 + C_{+\uparrow} \exp\left(\frac{-a}{\tau |v_z|}\right)\right) (1 - \mathcal{D}_{\uparrow}) - 1 \right] \exp\left(\frac{a}{\tau |v_z|}\right) \\
D_{+\downarrow} &= \left[\left(1 + C_{+\downarrow} \exp\left(\frac{-a}{\tau |v_z|}\right)\right) (1 - \mathcal{D}_{\downarrow}) - 1 \right] \exp\left(\frac{a}{\tau |v_z|}\right) \\
D_{-\uparrow} &= -\exp\left(\frac{-b}{\tau |v_z|}\right) \\
D_{-\downarrow} &= -\exp\left(\frac{-b}{\tau |v_z|}\right)
\end{aligned}$$

Appendix B

Calculation of the current density

The calculations leading to (35):

$$\begin{aligned}
\frac{\partial |\psi|^2}{\partial t} &= \frac{\partial(\psi^* \cdot \psi)}{\partial t} = \psi^* \frac{\partial \psi}{\partial t} + \frac{\partial \psi^*}{\partial t} \psi \\
&= \frac{i}{\hbar} (-\psi^* \hat{H} \psi + (\hat{H} \psi)^* \psi) \\
&= \frac{i}{\hbar} \left(-\psi^* \frac{\hat{p}_x^2}{2m_R^*} \psi + \left(\frac{\hat{p}_x^2}{2m_R^*} \psi \right)^* \psi - \psi^* \hat{p}_x A \psi + (\hat{p}_x A \psi)^* \psi \right) \\
&= \frac{1}{i\hbar} \left(\hat{p}_x \left[\psi^* \frac{\hat{p}_x}{2m_R^*} \psi + \psi \left(\frac{\hat{p}_x}{2m_R^*} \psi \right)^* \right] + \psi^* \hat{p}_x A \psi + \hat{p}_x \psi^* A \psi \right) \quad (\dagger) \\
&= \frac{\hat{p}_x}{i\hbar} \left(\psi^* \frac{\hat{p}_x}{2m_R^*} \psi + \psi \left(\frac{\hat{p}_x}{2m_R^*} \psi \right)^* + \psi^* A \psi \right) \\
&= \frac{\hat{p}_x}{i\hbar} \left(\psi^* \frac{\hat{p}_x}{2m_R^*} \psi + \psi \left(\frac{\hat{p}_x}{2m_R^*} \psi \right)^* + \frac{1}{2} (\psi^* A \psi + \psi (A \psi)^*) \right) \\
&= \frac{\hat{p}_x}{2i\hbar} \left(\psi^* \left(\frac{\hat{p}_x}{m_R^*} + A \right) \psi + \psi \left(\left(\frac{\hat{p}_x}{m_R^*} + A \right) \psi \right)^* \right) \quad (54)
\end{aligned}$$

Where in (\dagger) we have used that $\hat{p}_x^* = -\hat{p}_x$ and $(A\psi)^*\psi = \psi^*A\psi$ because A is Hermitian.